

International Commission for



the Northwest Atlantic Fisheries

Serial No. 5107  
(D.c.1)

ICNAF Res.Doc. 77/VI/54  
(Revised)

ANNUAL MEETING - JUNE 1977

Physical oceanography and the abiotic influence on cod recruitment in the Flemish Cap region

by

R.M. Hayes, D.G. Mountain, and T.C. Wolford  
US Coast Guard Oceanographic Unit  
Bldg. 159-E, Navy Yard Annex  
Washington, D.C. 20390

Abstract

Oceanographic station data from 1934 to 1976 archived for the Flemish Cap region (ICNAF Statistical Division 3M) of the Northwest Atlantic are limited in geographic distribution and consist mainly of depth, temperature and salinity observations made during April, May, and June. These observations indicate that all aspects of the oceanography of the Flemish Cap region exhibit considerable variation from year to year.

Changes in the path of the North Atlantic Current are shown to be consistent with a conservation of potential vorticity, while variations in the Labrador Current characteristics are related to atmospheric conditions. However, no satisfactory explanation is found for the changes in water properties on Flemish Cap.

A simple multiple linear regression analysis suggests that the significant factors influencing cod recruitment on Flemish Cap are the total cod population of Flemish Cap, meridional and zonal Ekman transports, and the mean April sea temperatures.

Introduction

At the request of the Chairman of the ICNAF Environmental Working Group, a study of the Flemish Cap region has been conducted by the authors using, in part, data collected at oceanographic stations by the US Coast Guard from 1934 to 1976. In addition, an attempt was made to identify the relationships between the year-class strengths of cod and various environmental factors, such as currents, water temperatures, and wind stress in the Flemish Cap region. An analysis of available data was made to determine, on a theoretical basis, why certain oceanographic features appear as they do on or near the Grand Banks of Newfoundland. At the same time, data requirements to fill the major gaps which existed in the knowledge of the area were identified.

Oceanographic Data Availability and Limitations

Since 1934 the International Ice Patrol has occupied approximately 11,000 oceanographic stations, out of a total of 14,219 occupied in the region, most of them near the Grand Banks of Newfoundland. The year 1934 was chosen as a starting point because field data collected during that year were considered to be of acceptable accuracy when compared with modern standards. Also, at that time, survey tracklines were established which are, in part, closely duplicated today. These tracklines were, and still are, designed to provide a geostrophic current velocity input to an operational iceberg drift model.

The location of the majority of icebergs varies monthly. In late March, many icebergs can generally be found south of 47° N latitude. Consequently, the majority of oceanographic stations occupied by the Ice Patrol were south of the Flemish Cap (47° N, 45° W) region. Later in the ice season, icebergs can be found farther north along the northeastern slope of the Grand Banks of Newfoundland. Therefore, in some years, an oceanographic survey was conducted, roughly in the region Cape Bonavista, Newfoundland - 46° W, 47° N-50° N, following the eastward branch of the Labrador Current (Fig. 1). As a result, most of the Ice Patrol oceanographic data tend to come from stations concentrated to the southwest of Flemish Cap in April and May, with some shifting to the northwest of Flemish Cap during June and July. Very little oceanographic data are available from the semi-circle east of Flemish Cap. Naturally, there are some variations from these general guidelines caused by the more recent Ice Patrol practice of surveying in the van of the icebergs.

The parameter of interest to the International Ice Patrol is the geostrophic current computed from dynamic height values obtained from pairs of oceanographic stations. Therefore, the only observations routinely taken by the International Ice Patrol are salinity and temperature values as a function of pressure, i.e., depth. Accordingly, very little oceanographic data obtained by the Ice Patrol were analyzed for nutrients or dissolved oxygen.

All of the Ice Patrol data collected since 1931 have been archived in the National Oceanographic Data Center (NODC), and are, therefore, readily available to the international oceanographic community. An inventory of the NODC data from 812 stations with measurements of the dissolved oxygen, phosphate, total phosphorous, nitrate, nitrite and silicate parameters was prepared in 1977 for the region 37° N-56° N, 42° W-55° W. The only comprehensive nutrient measurements listed from the Flemish Cap region were those made by the USSR in 1960 and published by Ponomarenko and Istoshina (1962).

Another NODC parameter inventory listing was requested for all oceanographic stations in the Flemish Cap region (46° N-49° N, 43° W-47° W). A total of 1,778 oceanographic stations were listed, the majority of which were occupied by the US Coast Guard during March through July.

A station listing consisting of 221 oceanographic stations was also prepared by NODC for the cod spawning area (46° N-47° N, 45° W-46° W). No dissolved oxygen or nutrient data were available.

An NODC plot of subsurface current data from the region, 37° N-50° N, 40° W-50° W, showed that, of 12 direct current measurements available as of 15 March 1976, none were made in the Flemish Cap region.

In 1976, upon request, the Canadian Marine Environmental Data Service produced a horizontal plot of dissolved oxygen data from eight depths for April of all years (Fig. 2-9).

The availability of mechanical (MBT) and expendable (XBT) bathythermograph data was determined for the United States (NODC) and Canada (MEDS). The bathythermograph data are not presently interchanged because of different digitization schemes. MEDS files have data from 5,078 MBTs and 83 XBTs for the Grand Banks region. The NODC files have data from 15,211 MBTs and 1,707 XBTs taken in the region 40° N-50° N, 41° W-55° W. Consequently, there is a large backlog of low accuracy temperature data available covering the interval 1955 to 1977.

Examples of products which are currently available from NODC are horizontal plots of monthly mean temperature and salinity data at any pre-selected depth (Fig. 10-27). Similar plots for chemical or biological parameters cannot be routinely drawn because of the paucity of the data.

All of these efforts by the data archivers are laudable beginnings to the consolidation and standardization of diverse data sets; it remains that future efforts will be required to render products of use in the evaluation of the abiotic influences on the health, stability, and production of fish stocks. Such products should emphasize the departure from the average physical environmental conditions for comparison with the immediate circumstances. The parameters chosen should have been experimentally proven to be relevant to year-class success.

A second, more serious shortcoming in the data record exists for the determination of indices of fish food production, i.e., nutrients, primary production, and secondary production, in the Newfoundland-Labrador region on a historically significant level. Within the range of abiotically-defined limiting factors, there purportedly lies a range of biotic density-dependent factors that control the size of populations. Knowledge of the availability of food for fish populations is particularly important during the post-spawning and larval drift periods. The relationship between the physical environment and the production of fish food may well provide the key to a predictive method for Flemish Cap groundfish recruitment estimation.

Finally, insufficient data on the flow of water on and near Flemish Cap do not permit an adequate assessment of the fate of eggs and larvae through drift or of the interchange of the water masses that determine the physical environment and the nutrient supply.

#### Circulation in the Region of the Grand Banks of Newfoundland

To understand the oceanography of Flemish Cap as it relates to cod and redfish, the physical oceanography of the Grand Banks of Newfoundland should be briefly examined. It may be succinctly summarized by presenting charts of the average dynamic topography based upon 32 years of oceanographic station data and a temperature-salinity diagram showing the three main water masses found near the Grand Banks (Fig. 28-30). The circulation, as indicated by these so-called normal charts, consists of the Labrador Current flowing southward between the 200- and 2,000-m isobath, indicating that bathymetric control is very important. Seaward, the North Atlantic Current meanders toward the north and east.

Between the North Atlantic Current and the Labrador Current is a denser water mass created by a mixing of water from the two currents. This mixed water mass, which varies in width, circulates cyclonically at varying speeds. The northeastward moving component of the mixed water is particularly significant to the oceanography of the Flemish Cap region. This water bathes the Beothuk Knoll and the southeastern quadrant

of Flemish Cap and has T-S characteristics which are favorable to the reported optimum temperature range of 3°C to 5°C for cod spawning, i.e., 4.3°C to 4.5°C temperatures with salinities of 34.6‰ to 34.9‰ from the 20-year averaged T-S curve for mixed water from 200 to 500 m (Fig. 31). The spawning cod should be able to adjust to variations in volume transports and position of the North Atlantic Current and the Labrador Current which might alter the environment from the optimum by changing their location by some few nautical miles.

What is not indicated by the normal dynamic height charts is the variability which occurs in the current patterns and water characteristics. This variability is discussed in the next section.

#### Labrador and Atlantic Current Variations

The purpose of this section is to consider the processes which control the physical oceanographic conditions in the Flemish Cap region. As mentioned above, Flemish Cap is bordered by two major current systems. The Labrador Current transports cold, low salinity water southward through Flemish Pass which lies to the west of the Cap, and along the eastern edge of the Grand Banks of Newfoundland. The warm, saline North Atlantic Current flows northeastward farther to the east, and passes to the south of Flemish Cap. The water on the Cap itself is essentially a mixture of the water from the two currents. The mean circulation pattern for the region is indicated by the average dynamic height distribution (Fig. 28). The deviations from the mean conditions, which are of primary interest here, will be discussed for both current systems and for the water properties on Flemish Cap.

#### The North Atlantic Current

The variations observed in the North Atlantic Current are primarily variations in the flow path, which is often characterized by large meanders and, occasionally, large current rings. These circulation patterns change significantly over a time scale of a month. Voorheis *et al.* (1973), investigating the temporal and spatial scales of the meanders and rings in the Grand Banks area, suggested a topographic steering of the North Atlantic Current. In this section, the variations in the path of the North Atlantic Current are shown to be consistent with a conservation of potential vorticity in which the topographic influence plays an important role. The vorticity equation for a barotropic, inviscid fluid may be written:

$$\frac{D}{Dt} \left[ \frac{f+\xi}{H} \right] = 0 \quad (1)$$

where the term in brackets is the potential vorticity,  $f$  is the Coriolis parameter,  $H$  is the water depth, and  $\xi$  is the relative vorticity. The relation implies that the potential vorticity remains constant along the flow path, i.e., is conserved. Expansion of the total derivative in (1) yields:

$$\frac{\partial \xi}{\partial t} + u \frac{\partial \xi}{\partial x} + v \frac{\partial \xi}{\partial y} + v \beta - \left( \frac{f+\xi}{H} \right) \left( u \frac{\partial H}{\partial x} + v \frac{\partial H}{\partial y} \right) = 0 \quad (2)$$

where  $\beta = \frac{\partial f}{\partial y}$ . The first term on the left is the local time change of relative vorticity, the next three terms are  $\frac{\partial \xi}{\partial y}$  the advection of vorticity, and the last term is the production of vorticity due to stretching. Assuming quasi-geostrophic flow, the velocities in (2) are derived from the dynamic height field,  $\psi$ , by:

$$u = - \frac{10}{f} \frac{\partial \psi}{\partial y} \quad ; \quad v = \frac{10}{f} \frac{\partial \psi}{\partial x}$$

and the relative vorticity in (1) by:

$$\xi = \frac{\partial v}{\partial x} - \frac{\partial u}{\partial y} = \frac{10}{f} \nabla^2 \psi \quad (3)$$

The dynamic height fields have been contoured and values interpolated to a 20-minute latitude by 20-minute longitude grid, allowing a simple five-point estimate of the Laplacian in equation (3) to be calculated. Using equation (3), the potential vorticity distribution will be calculated for data from two International Ice Patrol surveys which illustrate the variation in circulation pattern observed in the North Atlantic Current.

The potential vorticity and dynamic height distributions derived from data obtained by the International Ice Patrol in June 1964 are compared in Fig. 34. The dynamic heights indicate that the North Atlantic Current enters along the southern side of the survey area and heads northeastward. The flow curves to the northwest, then turns sharply clockwise forming a large anticyclonic meander. The potential vorticity distribution reveals a meander pattern similar in size, shape, and location to that in the geostrophic flow field. A very different situation was observed in April 1971 (Fig. 35). Then the current entered the region and headed northwestward, approximately parallel to the isobaths. The flow followed the bottom topography in a gradual clockwise turn leaving the region and heading northeastward

near 46° N, just south of Flemish Cap. The potential vorticity distribution follows the same pattern. Thus, in both years, the flow followed a path along which the potential vorticity remained nearly constant. The indication is that the North Atlantic Current conserves potential vorticity.

The process of vorticity conservation, through which equation (1) is approximately satisfied, is illustrated by comparing (Fig. 36) the potential vorticity, the relative vorticity and the water depth at points along the flow path in June 1964 (the crosses in Fig. 34). Initially the current flows toward deeper water and the potential vorticity decreases. The balance in equation (1) results in an increase in relative vorticity, turning the flow cyclonic (counterclockwise) toward the steep shelf break. With decreasing depth, the potential vorticity then rises, yielding a decrease in relative vorticity and an anticyclonic (clockwise) turning. This turning results in the large anticyclonic meander observed. The conservation process is essentially one of adjusting to changing water depth, i.e., a strong bathymetric steering.

Vorticity conservation during changes in the current path may be illustrated by showing that the local time change of relative vorticity ( $\frac{\partial \xi}{\partial t}$  in equation (2)) is consistent with observed changes. Using equation (2), the term, also called the  $\frac{\partial \xi}{\partial t}$  vorticity tendency, is calculated for data from May 1964, the month prior to the meander observation (Fig. 37). The vorticity tendency is positive (cyclonic) over the southwest half of the region and negative (anticyclonic) over the northeast portion. Considering the flow pattern observed in May 1964 (Fig. 37), these tendencies would cause a turning of the flow to the northwest over the southwestern half of the region, and to the southeast over the northeastern portion. The result would be an anticyclonic meander similar to that actually observed in June 1964 (Fig. 34).

The path of the North Atlantic Current appears to be controlled by a conservation of potential vorticity and to be subject to strong bathymetric steering. In 1971, the flow entered the survey area heading northwestward along the isobaths, and was able to follow smoothly the curving bottom topography. In 1964, the flow entered the survey area crossing the isobaths. The vorticity adjustment process interacted with the curving bottom topography to force the large meander. The difference between the two years was likely due to differences in the current path further upstream, perhaps the orientation of the current as it crossed the Newfoundland Ridge. Variation in the flow path could originate outside of the Grand Banks region and be advected into it under the constraint of vorticity conservation. The same conservation mechanism likely controls the current path further downstream. This could cause at least part of the North Atlantic Current to follow the isobaths counterclockwise around the east of Flemish Cap, as is perhaps indicated in the mean dynamic topography by the eastward flowing water between 49° and 50° N north of Flemish Cap. Water of North Atlantic Current origin (9.1°C, 34.90‰) was observed flowing eastward there on an International Ice Patrol cruise in May 1976.

#### Labrador Current

Unlike the North Atlantic Current, the path of the Labrador Current varies little in its position. The primary variations that are observed are in the volume and the temperature of the flow. Sufficient data do not exist to define accurately the seasonal variations, although earlier work by the Ice Patrol has noted a general decrease in the volume transport and an increase in the temperature of the Labrador Current from March through June (Bullard *et al.*, 1961). Of interest here will be the year-to-year variations of the volume flow and of the minimum observed temperature of the Labrador Current.

Volume transport. The average annual volume transports of the Labrador Current have been calculated from all Ice Patrol occupations of stations of Sections T and U for the period 1950-1964 and of Section A-3 for 1965-1976 (Fig. 38a). The transports have an average value of 3.6 Sv, with a range of 2.2 to 5.3 Sv. Low values were measured near the beginning and end of the period (1950-1953 and 1973-1976) with generally higher values during the intervening years. The method used to derive the volume transport involves the calculation of dynamic height values in areas where the water depth is shallower than the reference level (1,000 dbar). This requires the extrapolation of data into the Continental Shelf. This procedure is subjective and, when combined with the other inherent inaccuracies of the geostrophic assumption, yields expected errors in the transport values of perhaps  $\pm 30\%$ . Therefore, much of the year-to-year variation in the measured transport likely is not significant. However, the generally low values during 1950-1953 and 1967-1976 are probably indicative of below average Labrador Current transport.

Fofonoff and Ross (1962) introduced a method of calculating the theoretical wind-driven ocean transport from atmospheric pressure data by integrating the curl of the wind stress across the ocean. The method yields what is commonly called the Sverdrup transport. To satisfy continuity, the integrated transport across the ocean must be compensated by a western boundary current of equal magnitude and opposite direction. The Labrador Current is the western boundary current for the wind-driven subarctic gyre of the western North Atlantic Ocean and Labrador Sea. Using Fofonoff's method, the wind-driven transport of the North Atlantic Ocean has been calculated from monthly averaged surface pressure data for the period 1950-1963 (Fofonoff and Ross, 1962; Nasr and Wickett, 1974) and for 1964-1976 by the authors (to be referred to collectively as FRBC data). The calculated transports of the Labrador Current at 50° N, 50° W ( $T_{50}$ ) have been averaged by year (Fig. 38b).

The latitude of the zero transport contour ( $L_0$ ) along the 45° W meridian has also been calculated (Fig. 38c) to indicate the boundary between the cyclonic subarctic gyre and the anticyclonic gyre, and

thus represents the southern limit of the calculated Labrador Current.

The calculated transport values indicate that the wind stress over the North Atlantic Ocean is sufficient to drive a southward flowing western boundary current equal to or greater in magnitude than the measured Labrador Current. Similar calculations for the Gulf Stream system yield values less than or almost equal to the estimated volume transport of the Stream (Leetma *et al.*, 1977). The  $L_0$  series exhibits a close inverse relationship to  $T_{50}$ , implying that variations in the transport value are not due to changes in the strength of the subarctic gyre, but primarily to the north-south movement of the gyre's southern limit. This southern limit is generally near the latitude of Flemish Cap, and its movement occasionally results in a northward flowing boundary current to be calculated at  $50^\circ$  N (negative  $T_{50}$  values). While many of the year-to-year changes in the calculated transport probably are not significant, major changes in wind-forcing do occur which persist for three or more years. Two examples are the periods 1951-1953 and 1967-1976 (eight of the ten years) when  $L_0$  moved above  $50^\circ$  N yielding negative  $T_{50}$  values. Can the response of the ocean to these types of changes in atmospheric-forcing be observed? The variations in  $T_{50}$  do not closely follow those in the volume transport measured by the International Ice Patrol. While the two series are similar for the period 1950-1961, they exhibit a more nearly inverse relationship from 1962-1976.

By using various averaging and lagging schemes on monthly  $T_{50}$  values, a better correspondence may be obtained between the measured and calculated transports, but a consistent relationship cannot be found.

A close similarity between the measured and calculated transports is not to be expected. The time scale of the oceanic response to changing atmospheric-forcing varies on the order of a month for a purely barotropic mode, to a decade for a baroclinic response. As the total response would be a combination of these two modes, all patterns in the adjustment in the Labrador Current would likely be indiscernible, except for that resulting from changes in forcing that persist for a number of years. The recently-measured low Labrador Current transport may be an example of this type of adjustment, resulting from the northward movement of the subarctic gyre boundary during the past ten years.

Minimum temperature. The minimum temperatures measured in the Labrador Current have been averaged annually for all occupations of Sections T and U or A-3 for the period 1950-1976 (Fig. 39a). The temperatures are generally about  $-1.0^\circ\text{C}$  although variable with extremes of  $-1.7^\circ\text{C}$  in 1950 to  $+1.2^\circ\text{C}$  in 1966. The variations in the series do not resemble those of the transport series discussed above.

The high minimum temperature observed in 1958 has been attributed to advection and mixing of warmer offshore water into the Labrador Current along the coast of Labrador during January to March in response to the local winds (Dinsmore *et al.*, 1960). To extend this idea to other years, the southwest Ekman transports along the Labrador coast at  $55^\circ$  N,  $55^\circ$  W have been averaged for the months of January to March (Fig. 39b) from the same FRBC reports used in the transport discussion above. The series compares well with the minimum temperature data, suggesting that a large northeast Ekman transport (large negative values in Fig. 39b) reduces the influx of offshore water into the Labrador Current and preserves the low minimum temperature in the Current. The positive minimum temperatures in 1966 and 1971 are anomalous to this pattern and suggest that other factors, as yet undetermined, are also involved.

#### Flemish Cap Water Property Variations

To investigate the variation of water properties on Flemish Cap, a fairly small area on the southwest side ( $46^\circ40'\text{N}$ - $47^\circ00'\text{N}$ ,  $45^\circ00'\text{W}$ - $46^\circ00'\text{W}$ ) will be considered. The average temperature and salinity of the 0-200-m layer have been calculated annually for all Ice Patrol data from the period 1951-1976. No data were obtained in the region in 1950, 1966-1969, and 1975. On a temperature-salinity diagram, the results appear in two groups (Fig. 40a). The first group tends to be co-linear with a negative slope (warmer, low salt content to colder, high salt content). The points are generally in the mixed water region, but approach Labrador Current characteristics in the colder years. The variation in water properties does not appear to result from a varying mixing ratio of Labrador and North Atlantic Current waters which would yield a line with positive slope approximately along a constant density line. Instead, significant variation exists not only in water temperature (Fig. 40b) but also in density (Fig. 40c). The changes in density were generally observed throughout the water column and not in an isolated layer. The second group of points are from 1971-1974 and 1976, and are almost purely Labrador Current water. The large variation in water density suggests the occurrence of some form of upwelling in the Flemish Cap region.

For example, the water observed at the 200-m depth in 1957 and 1959 was characteristic of Labrador Current water from the 300-400-m depth. However, Flemish Cap is too deep to yield the type of wind-driven upwelling normally observed along a coast or a shelf break. Upwelling could result from a divergence of the wind-driven Ekman transport (Fofonoff and Dobson, 1963). Again using the FRBC reports, the vertical velocity driven by the divergence of the Ekman transport has been averaged for the months April to June for 1951 to 1976 at  $45^\circ$  N,  $45^\circ$  W (Fig. 41a). The results do not resemble closely the variations of water temperature or density, although a weak relation may exist by which lower density water is found during periods of lower upwelling velocities. The tendency toward Labrador Current properties on Flemish Cap in recent years could have resulted from a transport of water from the current toward Flemish Cap. However, the southeast Ekman transport at  $45^\circ$  N,  $45^\circ$  W, averaged for the months April to June (Fig. 41b), exhibits

no significant recent increase. The presence of Labrador Current water on Flemish Cap could be related to the northward movement of  $L_0$  during recent years, causing a larger portion of the Current to flow eastward along the north side of Flemish Cap instead of heading south along the eastern edge of the Grand Banks.

### Conclusions

All aspects of the oceanography of the Flemish Cap region exhibit considerable variation on a year-to-year basis. For both the North Atlantic and the Labrador Currents, the primary variations appear to result from forcing applied outside of the Flemish Cap or Grand Banks regions, and plausible forcing functions have been identified for the oceanographic parameters considered. However, the suggested relationships are not presented as representing direct, linear cause and effect, but are at best only indicative of the actual physical process involved.

The large variation in water properties on Flemish Cap indicates influx of water from different depths. No single forcing parameter exhibits similar variations. The characteristics of the water on Flemish Cap likely result from a complicated process, involving not only the local wind field, but also the conditions in the North Atlantic and the Labrador Currents. Hydrodynamic modeling will probably be required to account for the interaction of the various inputs or forcing functions affecting the oceanography of Flemish Cap.

### Climate and Recruitment of Cod on Flemish Cap, ICNAF Div. 3M

Stable fisheries populations exhibit natural fluctuations in numbers that can only be explained by variations in the environmental milieu. These variations in numbers represent the observed differences in year-class success that are determined by a combination of density-dependent and non-density-dependent controlling factors. Nowhere is this philosophy more succinctly stated than in Cushing (1973, p. 41): "Numbers are stabilized in the face of high environmental variability, which is reflected in the variation of recruitment. Indeed the latter may be a direct reflection of changes in the weather. Recruitment variation is, however, damped by the number of year-classes in adverse environments and by the stabilization mechanism in all environments. The population is thus insulated from the variation in the environment as expressed in stock numbers." The above reflects the mechanism of the long-term stability of numbers and not the events that determine year-class success. The variation in year-class strength may be seen in the estimated indices of abundance for cod (Wells, 1973).

A predictive relationship between gadoid recruitment and physical environmental parameters has long been sought (temperature: Hermann *et al.*, 1965, and Dickson, Pope and Holden, 1973; salinity: Dickson, 1971; and wind: Hill and Lee, 1957).

The contemporary hypothesis regarding the response of recruitment of certain demersal fish stocks to climatic change is that the maximum effect of climate occurs during the period from spawning to the end of the yolk-sac larval drift stage. The critical controlling mechanism is the essential match-up in time and space of the planktonic production cycle with the depletion of the larval yolk-sac such that successful year-classes are found when this match-up is closely coordinated.

The climatic factors that determine the onset of the late winter/spring primary production cycle are temperature, wind strength (mixing), wind direction (upwelling), and amount of incident solar radiation (Cushing, 1973, p. 37 and 149). Both the strength and direction contribute to the amount of biogenous material available for primary production through the process of upwelling and mixing. Another consequence of wind velocity might be a variation in volume flow of the types of water bathing the Flemish Cap, which would affect the timing of the production cycle. This is particularly critical considering the disparate nature of the water properties and nutrient content of the two water masses, the Labrador and North Atlantic Currents, which converge near this region (Ponomarenko and Istoshina, 1962).

The rate of primary production depends on the rate of development of the production ratio. The production ratio relates the compensation depth to the depth of mixing. The compensation depth is the depth where photosynthesis equals respiration when integrated over depth. Incident solar radiation and wind as it affects mixing, upwelling, and hence turbidity, are the major determinants of the compensation depth. The primary factors which determine larval yolk-sac depletion are the time of spawning and the temperature of the water during egg and larval drift.

Since spawning is fairly well fixed in time genetically and behaviorally, the adjustment mechanism, if one exists, would appear to be a delay in larval development to match a delay in the production cycle. Whenever the physical environment takes divergent directions for the critical parameters determining the production cycle and larval development (essentially temperature and wind for the Flemish Cap cod), the food supply becomes insufficient for the emergent larvae which consume their yolk-sacs, die, and contribute to a poor year-class. The density-dependent recruitment mechanisms mentioned before (Ricker, 1954) will compensate for the vagaries of climate in subsequent spawning periods to bring about the observed stability in numbers found in the overall abundance of this fishery. Yet, the results of an unsuccessful year-class can be followed as a cohort throughout its existence.

To test the hypothesis that climatic change can account for some of the variability in year-class success, a simple regression model was devised to quantify the relationship between the physical environment and recruitment for the cod stock on Flemish Cap (ICNAF Div. 3M) during a 9-year period in the 1960's. The model uses April measurements of mean sea temperature between 46°40'N to 47°00'N and 45°00'W to 47°00'W (0-200 m), meridional Ekman transport, zonal Ekman transport, and total cod population at the beginning of the year (from virtual population assessments) to predict the recruitment of young cod four years hence. The sea temperatures are taken from US Coast Guard International Ice Patrol Bulletins from 1955 to 1963. The Ekman transport values for the same years are from the FRBC reports referred to previously. All virtual population assessments of cod come from Wells (1973) and Templeman (1976). The temperature and transport data are calculated for April because this month has been shown to yield the greatest number of yolk-sac larvae near Flemish Cap (Templeman, 1976), and also appears to sustain the highest rate of primary production (Fedosov, 1962; Movchan, 1962).

This simple model is a multiple linear regression with four independent variables. The statistical computations were carried out on a CDC-3300 computer using a program written by one of the authors. The methodology employed, the so-called "Abbreviated Doolittle or Gauss-Doolittle Method" is named after the man who introduced this procedure in 1878 while an engineer with the US Coast and Geodetic Survey (Steel and Torrie, 1960). The multiple linear regression equation takes the form:

$$R_{4 \text{ yrs}} = a + b_1 Vt + b_2 Ta + b_3 Wm + b_4 Wz$$

where:

$$\begin{aligned} Vt &= \text{total population (from virtual population assessment) (x } 10^7) \\ Ta &= \text{mean April sea temperature Flemish Cap (}^\circ\text{C)} \\ Wm &= \text{meridional Ekman transport on Flemish Cap (} 10^3 \text{ metric tons/sec/km)} \\ Wz &= \text{zonal Ekman transport on Flemish Cap (} 10^3 \text{ metric tons/sec/km)} \\ R_{4 \text{ yrs}} &= \text{total population of 4-year-old cod four years hence (x } 10^7). \end{aligned}$$

The parameters  $Vt$ ,  $Ta$ ,  $Wz$ , and  $Wm$  are calculated for 1955-1963 inclusive.  $R_{4 \text{ yrs}}$  is predicted for 1959 to 1967 inclusive. For the above-mentioned years, the regression coefficients are:

$$R_{4 \text{ yrs}} = -2.2247 + 0.1390 Vt + 0.9664 Ta + 0.2301 Wm + 1.0392 Wz .$$

The reduction in sums of squares attributable to regression was tested for significance and was found significant at  $0.10 > P > 0.05$ . The multiple correlation coefficient for the data is + 0.91 which is significant at  $0.10 > P > 0.05$ . The standard error of the estimate of recruitment is  $1.32 \times 10^7$  cod. The 95% confidence limits for the partial regression coefficients are listed below:

$$\begin{aligned} b_1 &= 0.1390 \pm 0.3859 \\ b_2 &= 0.9664 \pm 2.6827 \\ b_3 &= 0.2301 \pm 0.6388 \\ b_4 &= 1.0392 \pm 2.8848 \end{aligned}$$

A graphical comparison was made between the actual 4th year-class cod recruitment and that calculated by the regression equation (Fig. 42).

The test of the effectiveness of a model is how well it predicts the future. This would require a data set for cod populations, Ekman transports, and sea temperatures for some other period of which only the temperature data were available to the authors at the time of writing this paper. Nevertheless, the true value of a model lies in its ability to indicate the applicability of a particular fishery theorem to a stock of interest; and most importantly, a model allows the investigator to identify any data gaps that hinder the more precise description of the system under study. In this case, it is difficult to say whether the unexplained residuals in regression are the result of an imperfect data set or an overlooked independent variable. The danger of drawing hasty conclusions from such small data sets is well known. Notwithstanding, this exercise has shown that it may be possible to explain some of the variability of year-class success for ICNAF Div. 3M cod with a small amount of readily available physical environmental data. This analysis shows that recruitment of 4-year-old cod in this area for this period increased with increasing total population size, increasing temperature, with decreasing southerly Ekman transport, and increasing easterly Ekman transport.

The path to a more precise model leads toward a hybrid model which combines density-dependent and non-density-dependent factors to account for both the influence of climate and fishing on recruitment. In turn, variations in recruitment determined from the above would serve as a base for further analysis that would follow a density-dependent (Ricker type) recruitment curve related to parental stock size, which has been shown to be operative for fish stocks similar to the one studied here.

The following recommendations are made concerning the evaluation of climatic factors and year-class

strength of Flemish Cap cod: (1) obtain a data set from 1968 to the present containing age-class indices of abundance for Flemish Cap cod, April mean sea temperature of the surface strata, and meridional and zonal Ekman transport - all of which are necessary to test the validity of the multiple linear regression model presented herein; (2) if the model indicates that all the essential climatic factors governing Flemish Cap cod recruitment are accounted for, an investigation to better determine the timing of the production cycle and the spawning cycle should be undertaken; and (3) the appropriate physical factors controlling the production cycle (from (2) above) should be developed into a quantifying relationship such that a more precise approximation of recruitment would be possible.

#### References

- Bullard, R.P., R.P. Dinsmore, A.P. Franceschetti, P.A. Morrill, and Floyd M. Soule. 1961. Report of the International Ice Patrol Service in the North Atlantic Ocean - Season of 1960. *US Coast Guard Bulletin* No. 46, CG-188-15.
- Cushing, D.H. 1973. Recruitment and parent stock in fishes. *Washington Sea Grant Program*, WSG 73-1. 197 p.
- Dinsmore, R.P., R.M. Morse, and Floyd M. Soule. 1960. International Ice Patrol Service in the North Atlantic Ocean - The Season of 1958. *US Coast Guard Bulletin* No. 44, CG-188-13.
- Dickson, R.R. 1971. A recurrent and persistent pressure-anomaly pattern as the principal cause of intermediate scale hydrographic variation in the European Shelf seas. *Deutsche Hydrogr. Zeit.* 24(3):97-119.
- Dickson, R.R., J.G. Pope, and M.J. Holden. 1973. Environmental influences on the survival of North Sea cod. *In: The Early Life History of Fish.* J.H.S. Baxter, Editor, Springer-Verlag, Berlin, Heidelberg, New York 1974: 69-80.
- Fedosov, M.V. 1962. Investigation of formation conditions of primary productivity in the Northwest Atlantic. *In: Soviet Fisheries Investigations in the Northwest Atlantic*, Y.Y. Marti, ed. VNIRO-PINRO, Moskva. (Transl. for US Nat. Sci. Found., Washington, D.C. by Israel Prog. Sci. Transl., 1963): 125-135.
- Fofonoff, N.P., and C.K. Ross. 1962. Transport computations for the North Atlantic Ocean. *Fish. Res. Bd. Canada Manuscript Report Series* (Nos. 112, 114-124).
- Fofonoff, N.P., and F.W. Dobson. 1963. Transport computations for the North Pacific Ocean, 1955-1960. *Fish. Res. Bd. Canada Manuscript Report Series* No. 166.
- Hermann, F., P.M. Hansen, and Sv.Aa. Horsted. 1965. The effect of temperature and currents on the distribution and survival of cod larvae at West Greenland. *ICNAF Spec. Publ.* No. 6: 389-395.
- Hill, H.W., and A.J. Lee. 1957. The effect of wind on water transport in the region of the Bear Island fishery. *Proc. Roy. Soc. B.* 148: 104-116.
- Leetma, A., Pearn Niller, and Henry Stommel. 1977. Does the Sverdrup relation account for the Mid-Atlantic circulation? *J. Mar. Res.* 35: 1-10.
- Movchan, O.A. 1962. Quantitative development of the phytoplankton in the areas of the Newfoundland and Flemish Cap Banks and in adjacent waters. *In: Soviet Fisheries Investigations in the Northwest Atlantic*, Y.Y. Marti, ed. VNIRO-PINRO, Moskva (Transl. for US Nat. Sci. Found., Washington, D.C. by Israel Prog. Sci. Transl., 1963): 205-213.
- Nasr, J., and W.P. Wickett. 1974. Transport computations for the North Atlantic Ocean. *Mar. Env. Data Serv. Tech. Reports* Nos. 1-2.
- Ponomarenko, L.S., and M.A. Istoshina. 1962. Hydrochemical studies in the Newfoundland area. *In: Soviet Fisheries Investigations in the Northwest Atlantic*, Y.Y. Marti, ed., VNIRO-PINRO, Moskva (Transl. for US Nat. Sci. Found., Washington, D.C. by Israel Prog. Sci. Transl., 1963): 113-124.
- Ricker, W.E. 1954. Stock and recruitment. *J. Fish. Res. Bd. Canada*, 11(5): 559-623.
- Scobie, R.W., and R.H. Schultz. 1976. Oceanography of the Grand Banks region of Newfoundland, March 1971-December 1972. CG 373-70.
- Steel, R.G.D., and J.H. Torrie. 1960. Principles and procedures of statistics with special reference to the biological sciences. McGraw-Hill Book Co., Inc., N.Y., Toronto, London: 290-304.
- Templeman, W. 1976. Biological and oceanographic background of Flemish Cap as an area for research on the reasons for year-class success and failure in cod and redfish. *ICNAF Res. Bull.* No. 12: 91-117.

US Coast Guard International Ice Patrol Bulletins. 1955-1963. CG-188 No. 41-49. US Dept. of Transportation, Washington, D.C.

Voorheis, G.M., K. Aggaard, and L.K. Coachman. 1973. Circulation patterns near the Tail of the Grand Banks. *J. Phy. Oceanogr.*, 3: 397-405.

Wells, R. 1973. Virtual population assessment of the cod stock in ICNAF Div. 3M. *ICNAF Res.Doc.* 73/105, Serial No. 3068.

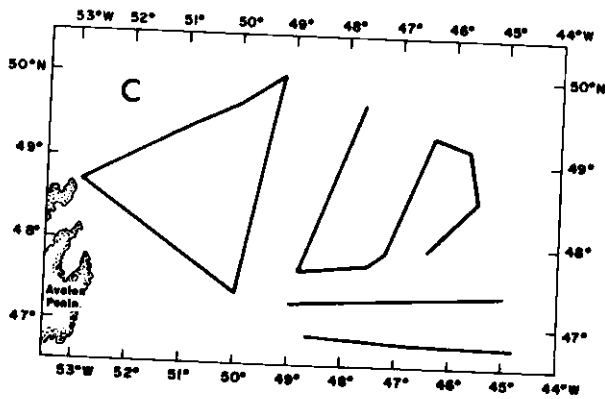
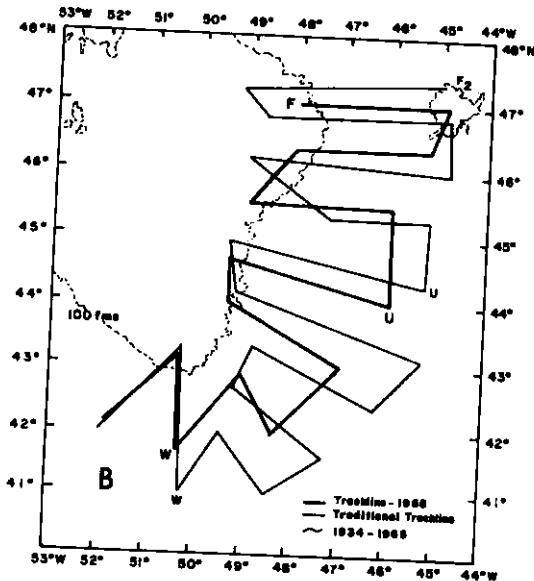
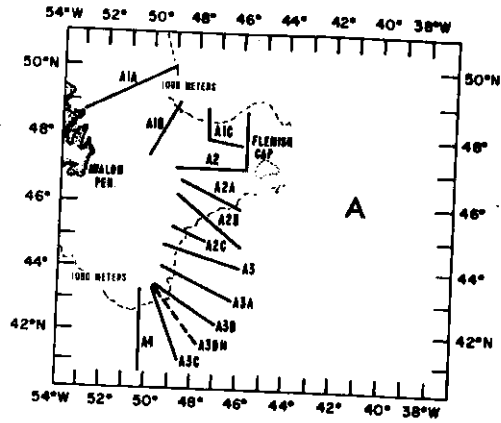


Fig. 1A. International Ice Patrol standard sections in use from 1969 to present.

Fig. 1B. Survey tracklines in use from about 1934 until 1965.

Fig. 1C. Survey tracklines occupied from about 1948 until 1965. These were generally occupied late in the ice season (~ June or July) when the icebergs have retreated to the north.

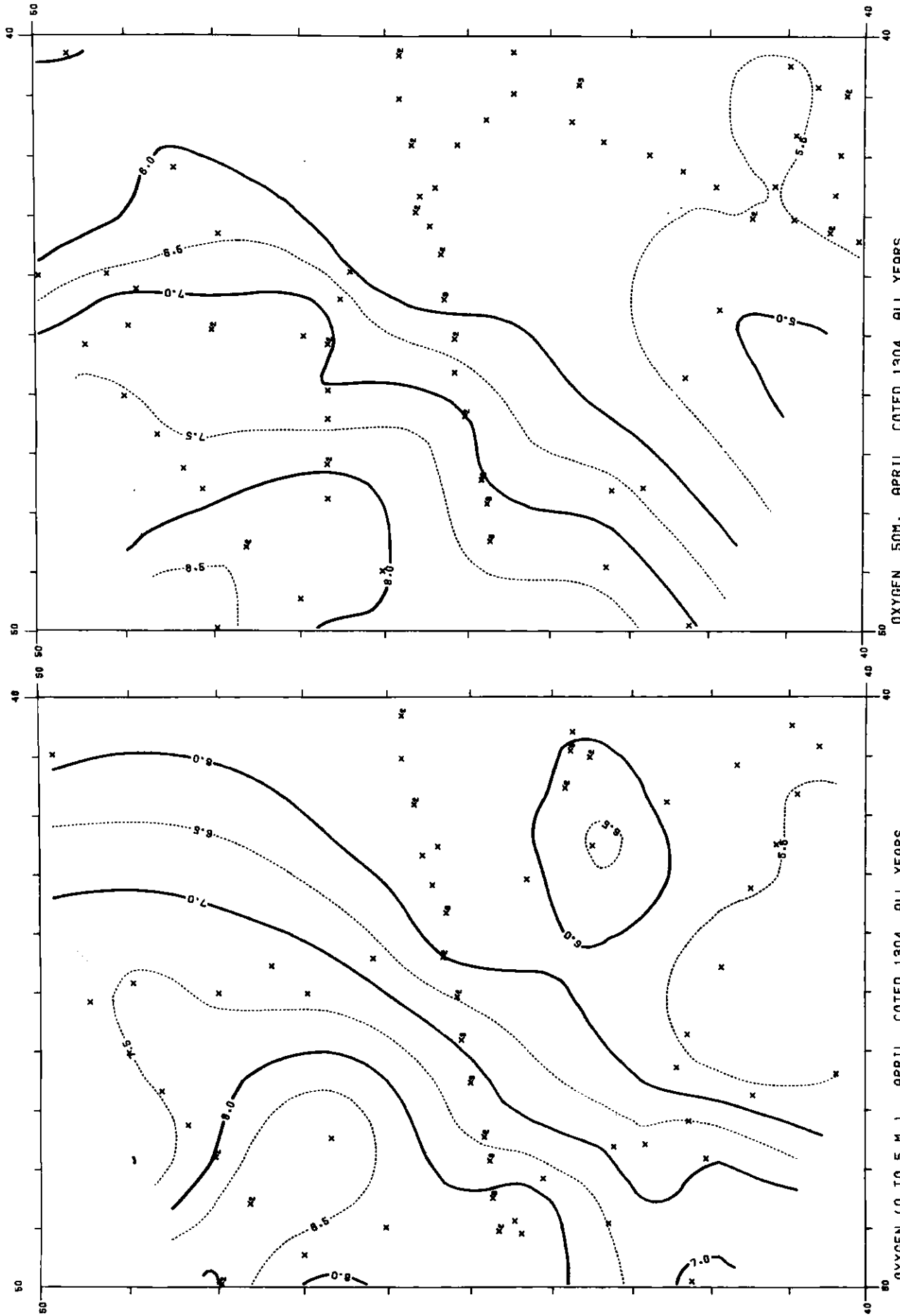
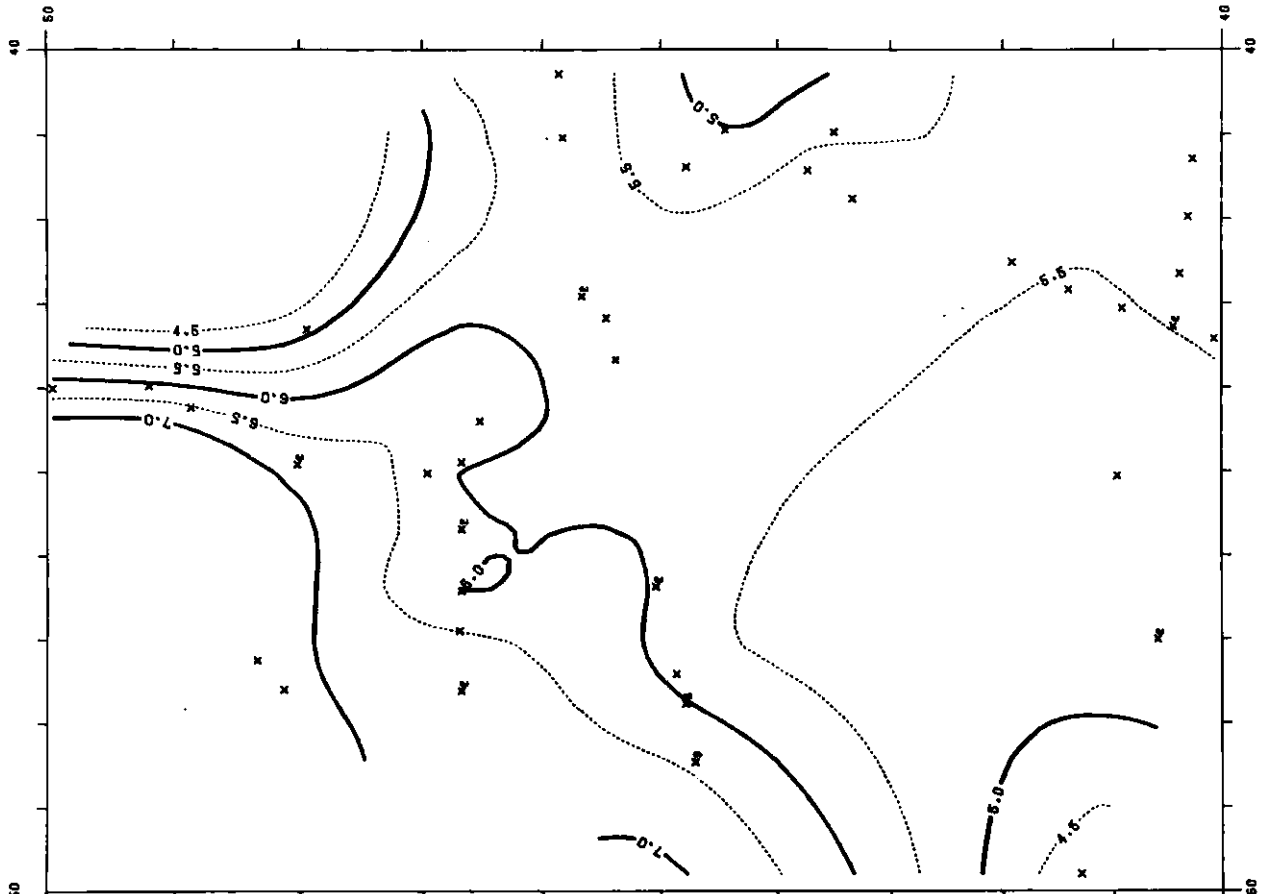
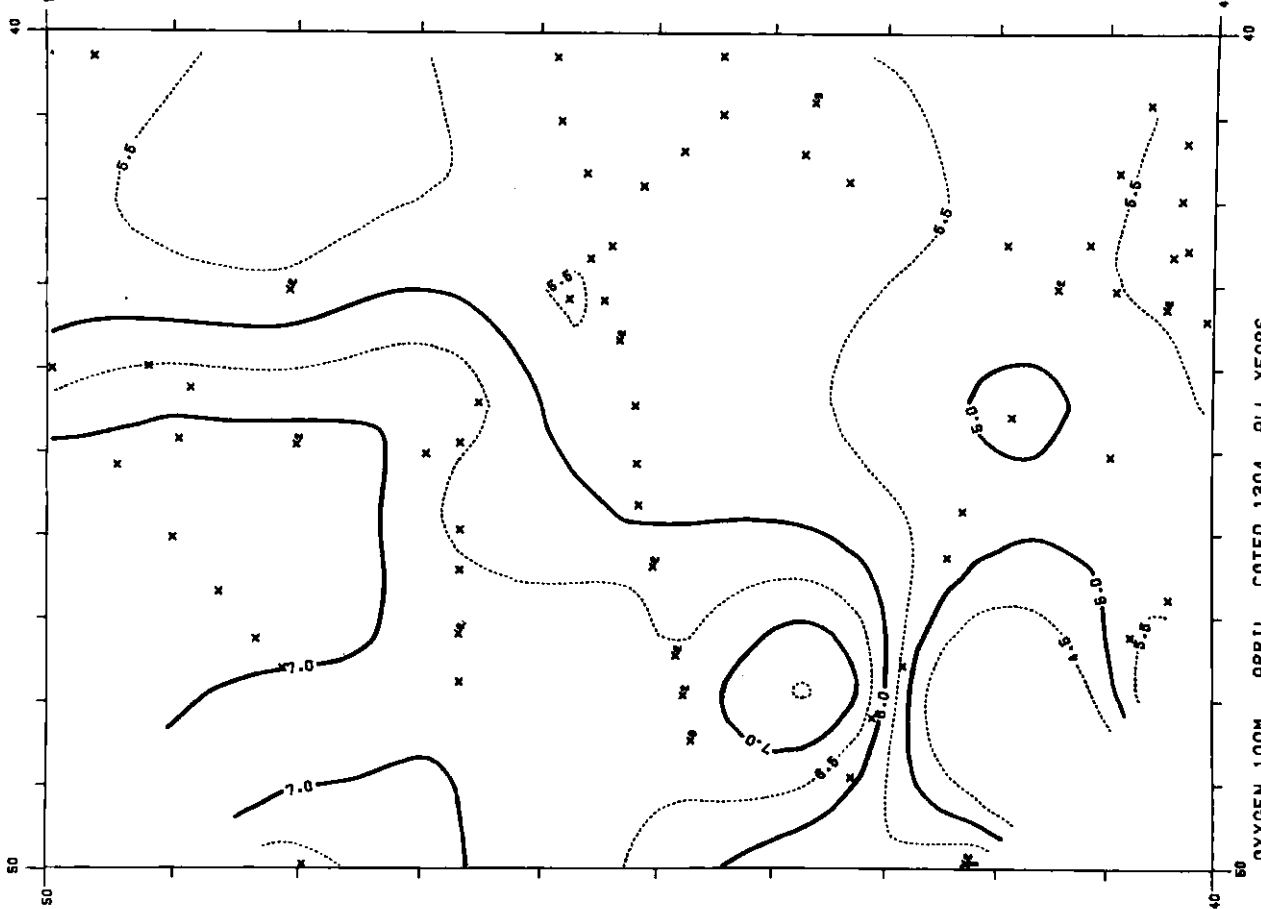


Figure 2. Horizontal plot of surface dissolved oxygen based upon data collected in April from all years.

Figure 3. Horizontal plot of 50 meters dissolved oxygen based upon data collected in April from all years.



OXYGEN 150M. APRIL COTED 1304 ALL YEARS



OXYGEN 100M. APRIL COTED 1304 ALL YEARS

Figure 5. Horizontal plot of 150 meters dissolved oxygen based upon data collected in April from all years.

Figure 4. Horizontal plot of 100 meters dissolved oxygen based upon data collected in April from all years.

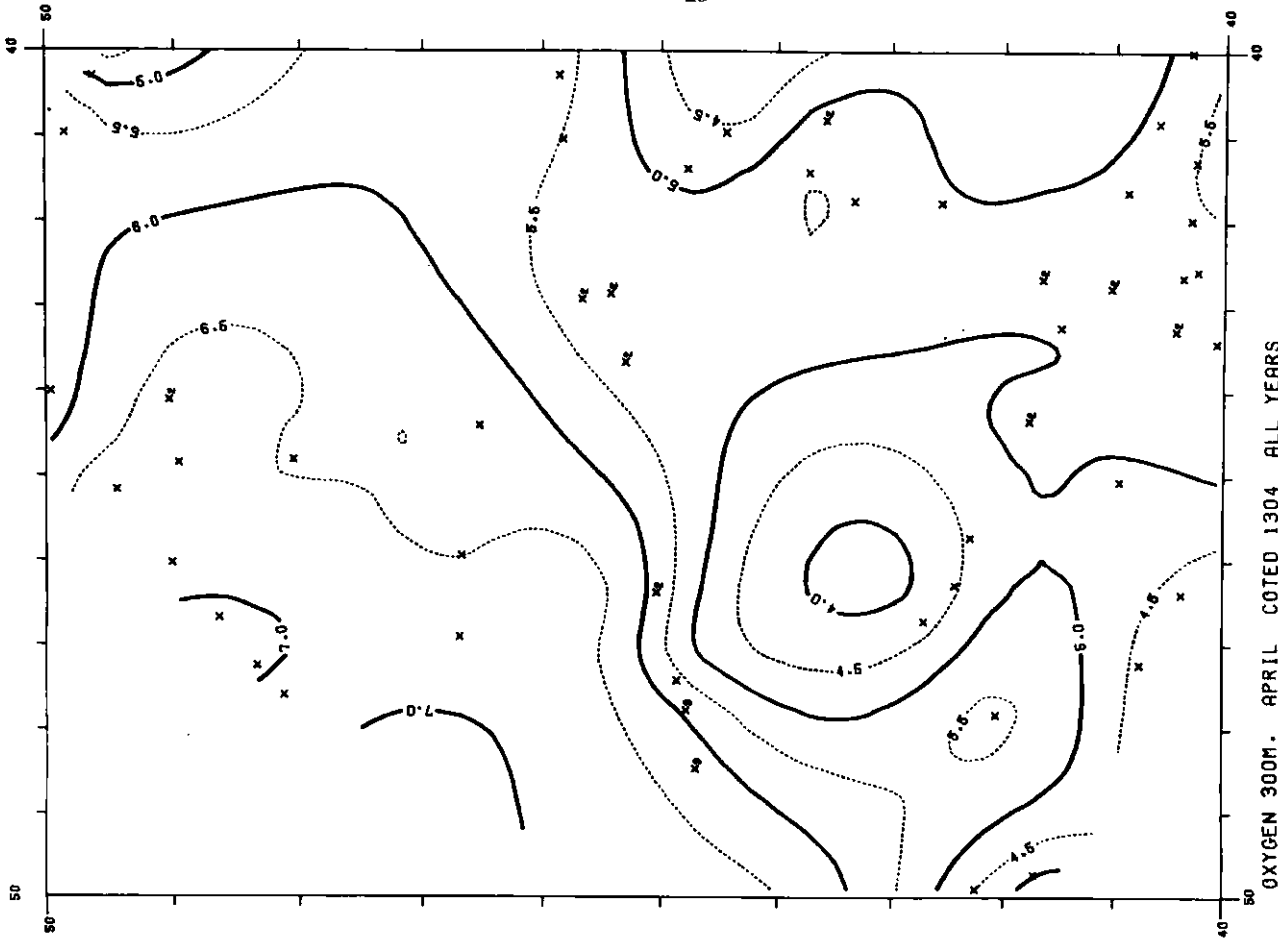


Figure 7. Horizontal plot of 300 meters dissolved oxygen based upon data collected in April from all years.

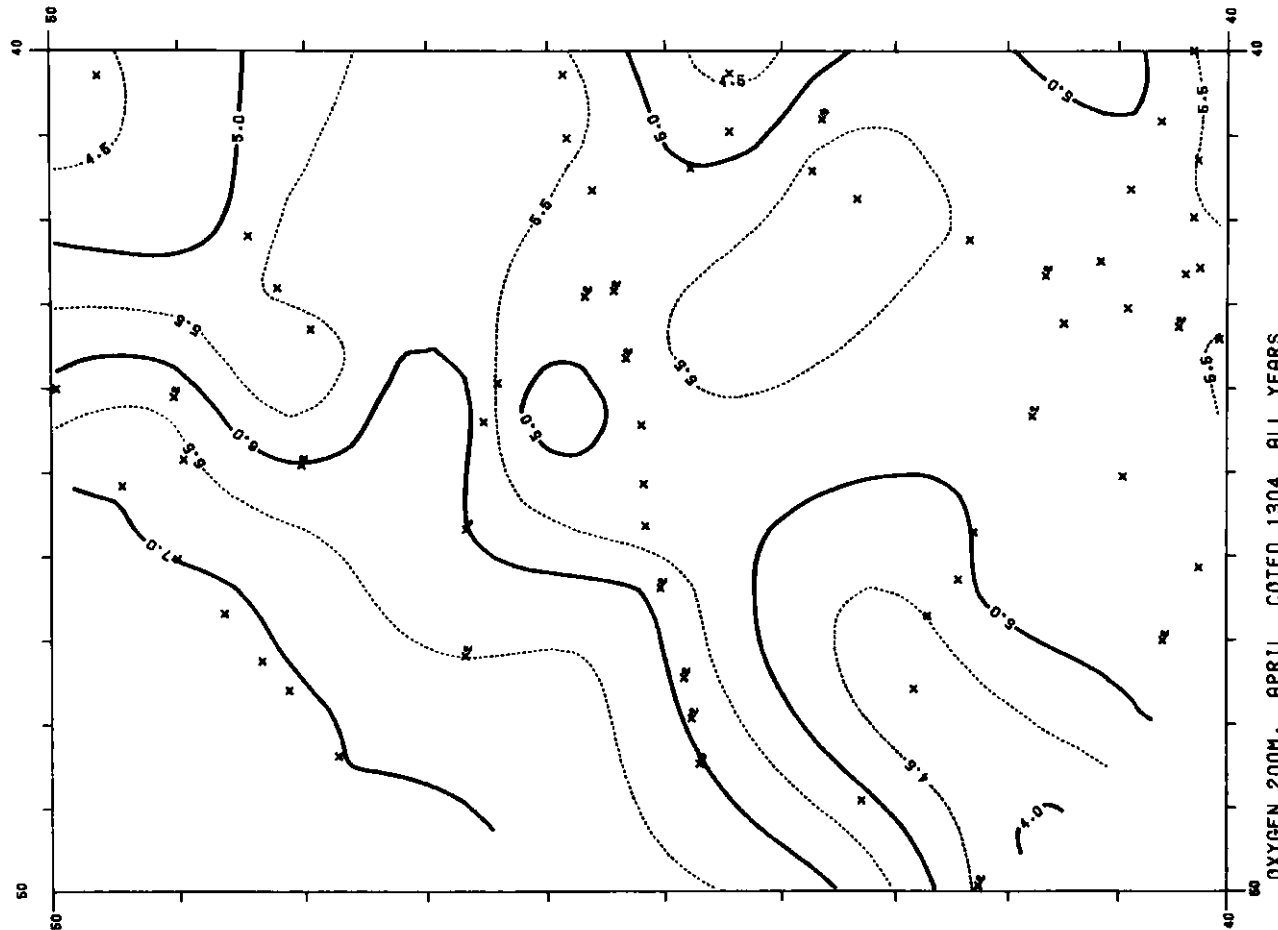
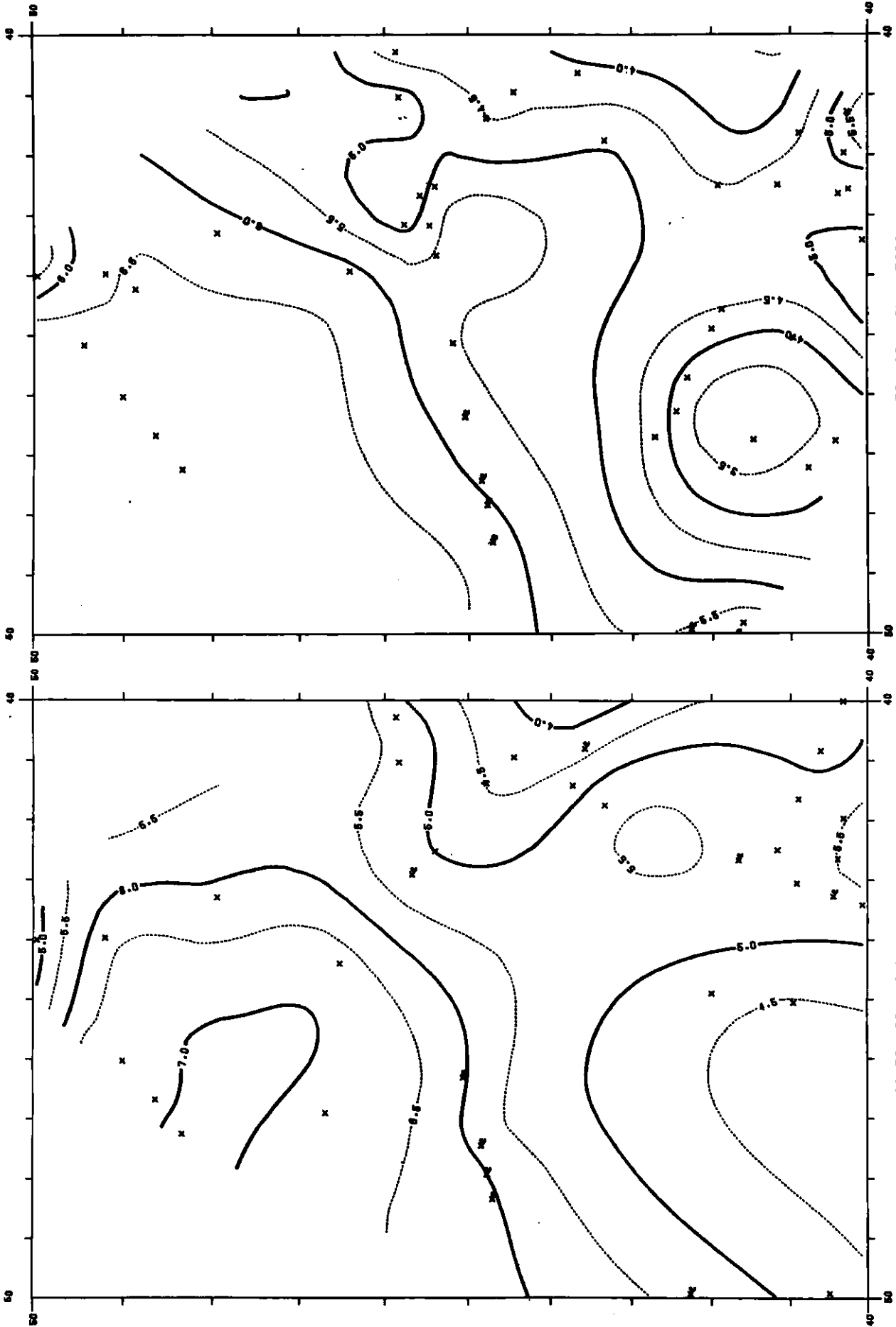
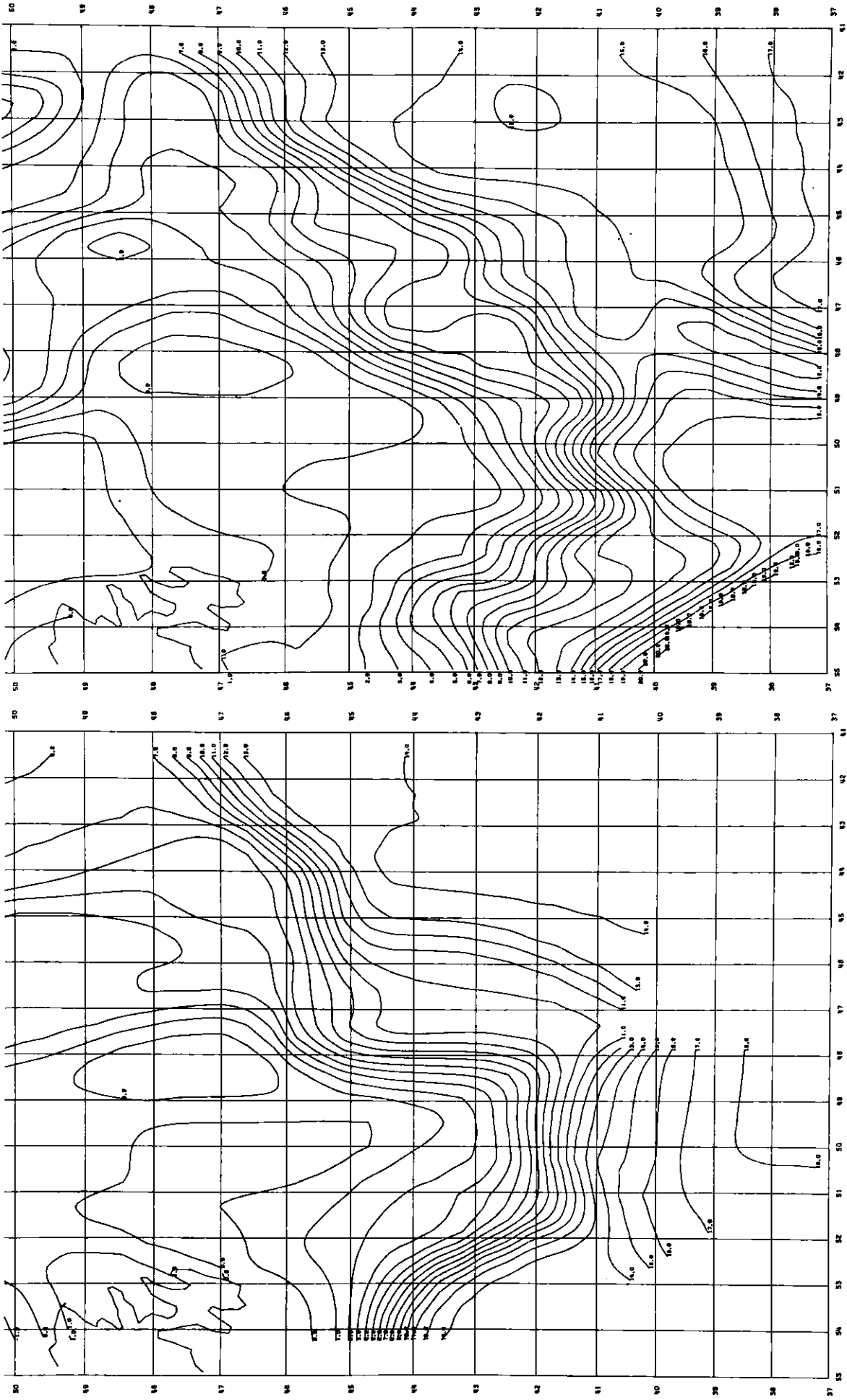


Figure 6. Horizontal plot of 200 meters dissolved oxygen based upon data collected in April from all years.



OXYGEN 495M. APRIL COTED 1904 ALL YEARS  
Figure 9. Horizontal plot of 495 meters dissolved oxygen based upon data collected in April from all years.

OXYGEN 400M. APRIL COTED 1904 ALL YEARS  
Figure 8. Horizontal plot of 400 meters dissolved oxygen based upon data collected in April from all years.

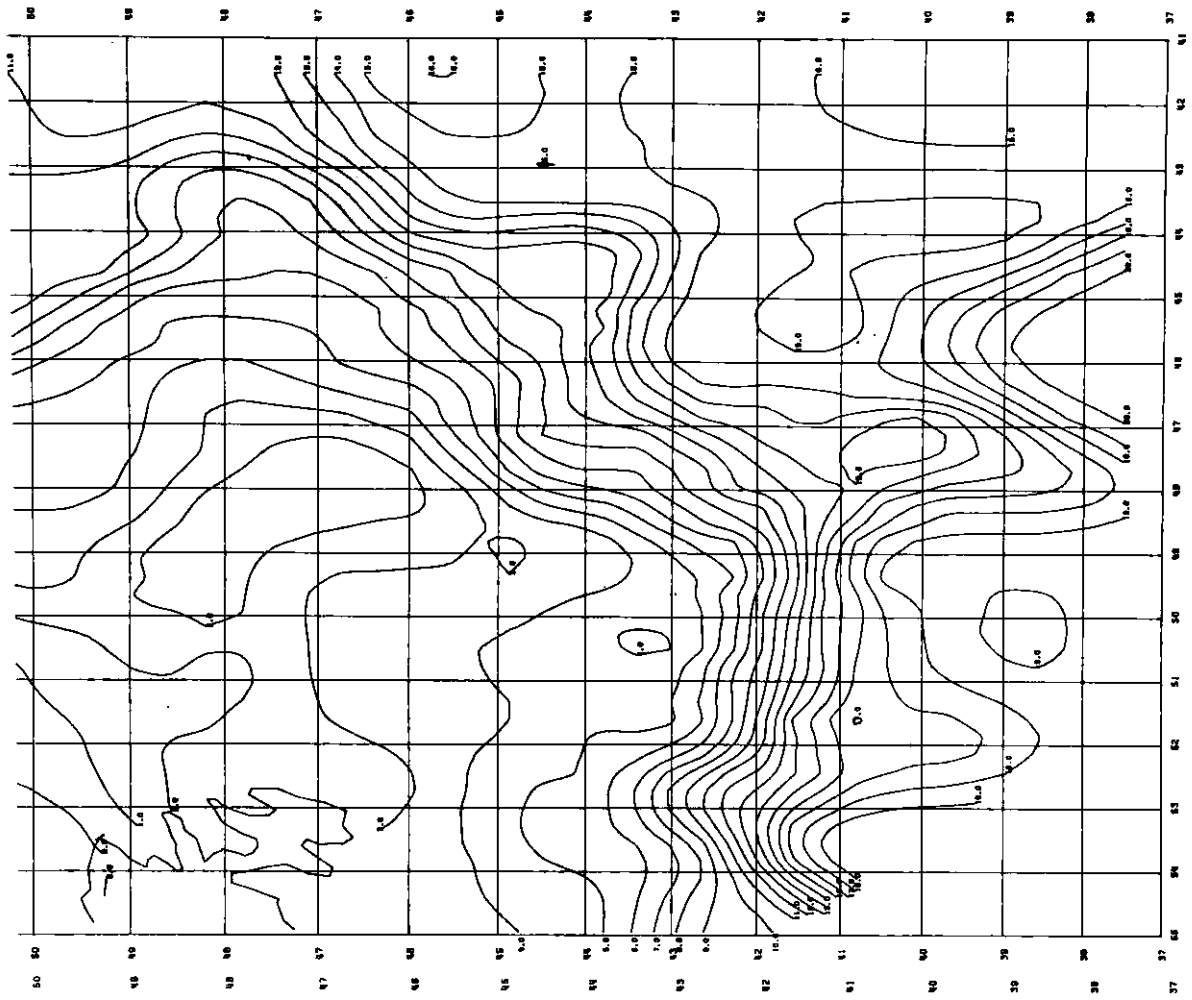


ICMRF AREA SURFACE TEMPERATURE

Figure 10. Horizontal plot of mean sea surface temperature for February.

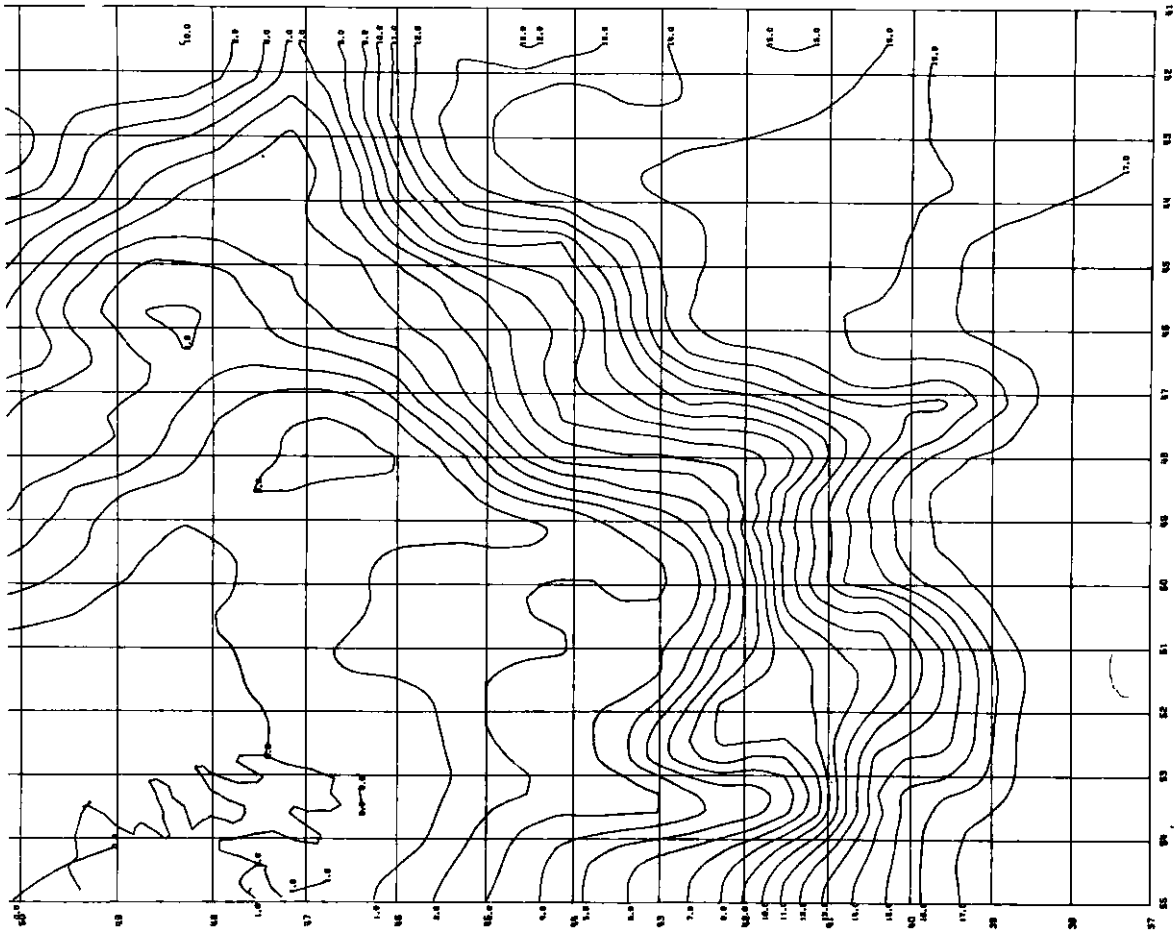
ICMRF AREA SURFACE TEMPERATURE

Figure 11. Horizontal plot of mean sea surface temperature for March.



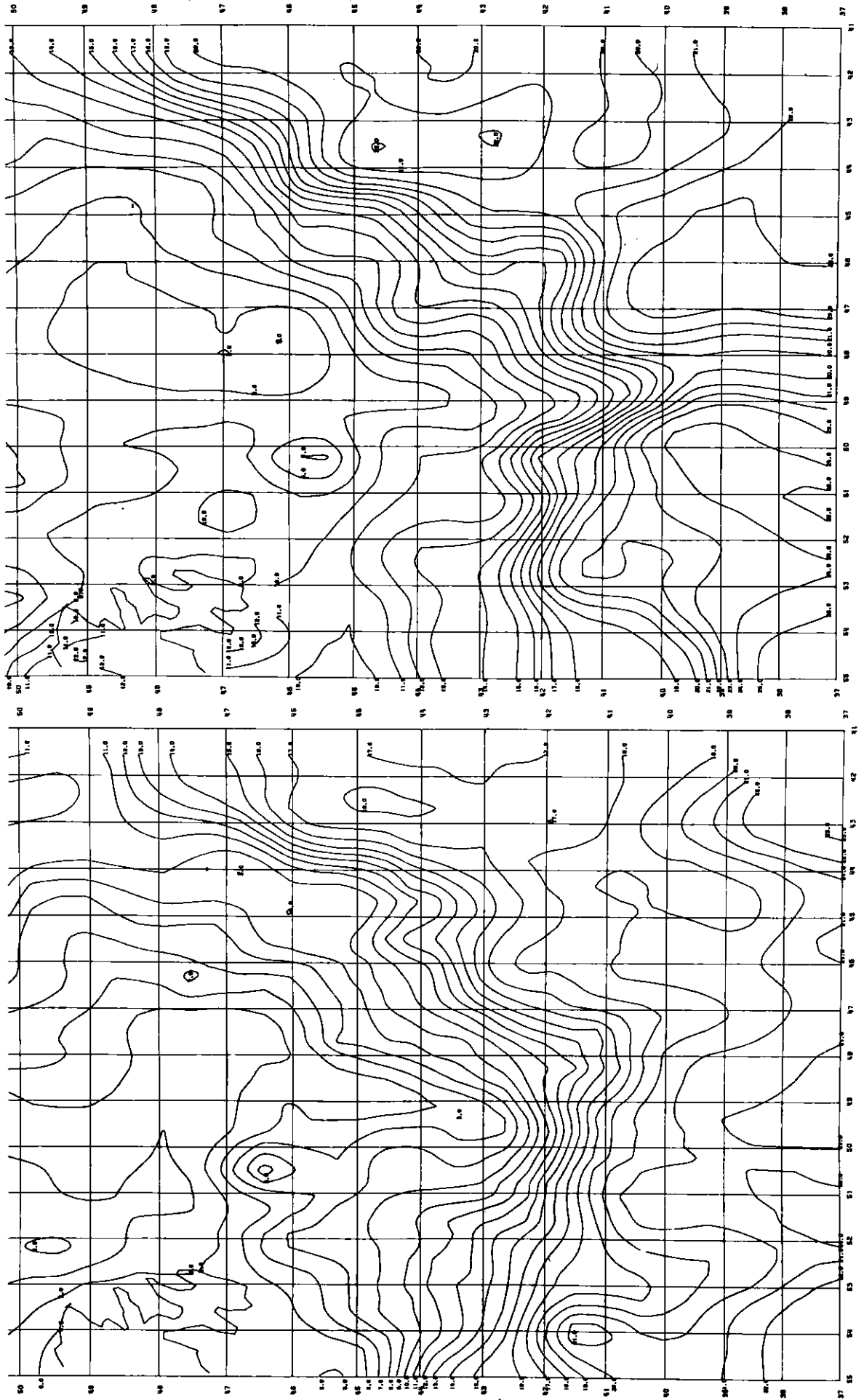
ICRAF AREA SURFACE TEMPERATURE

Figure 13. Horizontal plot of mean sea surface temperature for May.



ICRAF AREA SURFACE TEMPERATURE

Figure 12. Horizontal plot of mean sea surface temperature for April.

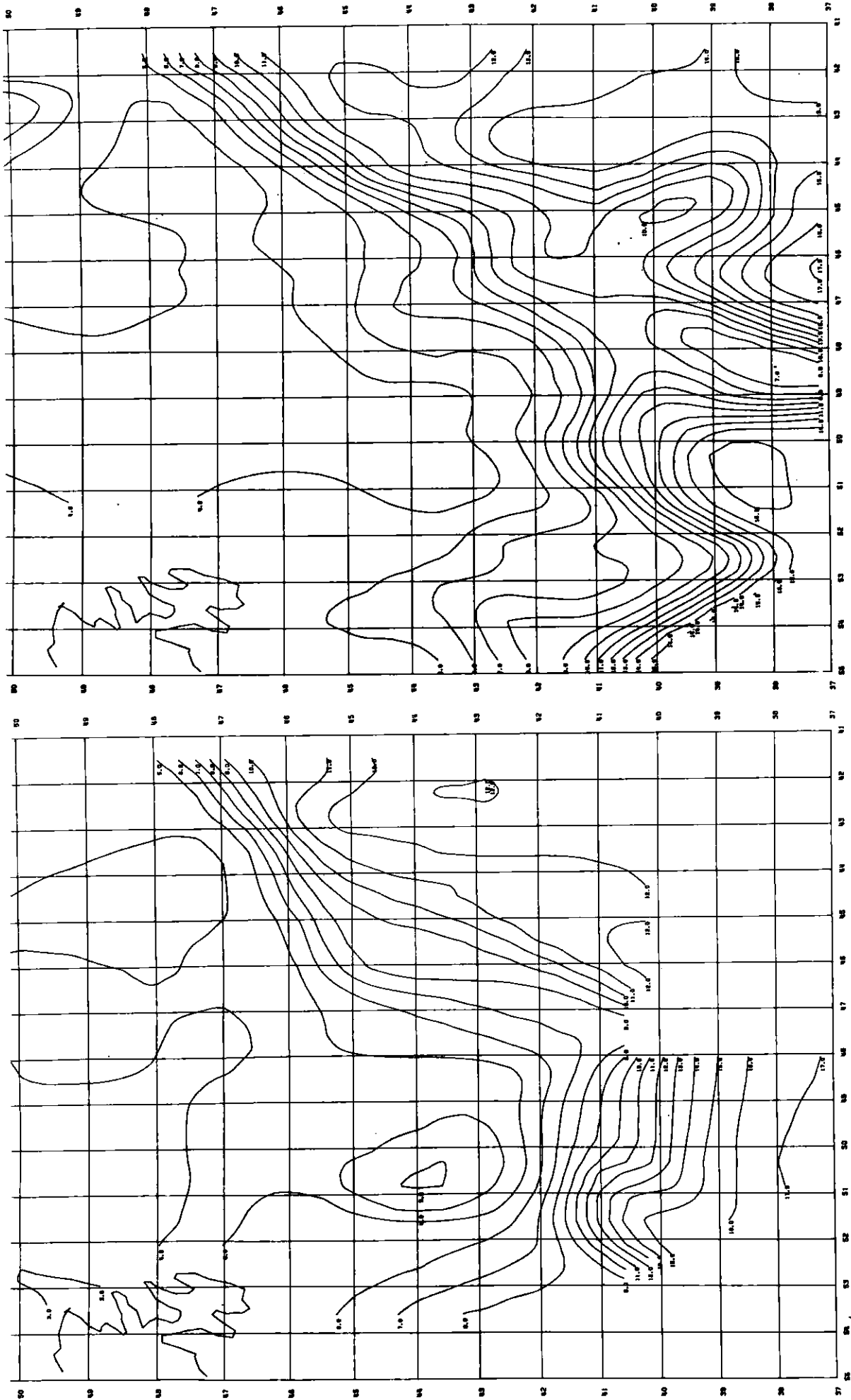


ICMAP AREA SURFACE TEMPERATURE

Figure 15. Horizontal plot of mean sea surface temperature for July.

ICMAP AREA SURFACE TEMPERATURE

Figure 14. Horizontal plot of mean sea surface temperature for June.

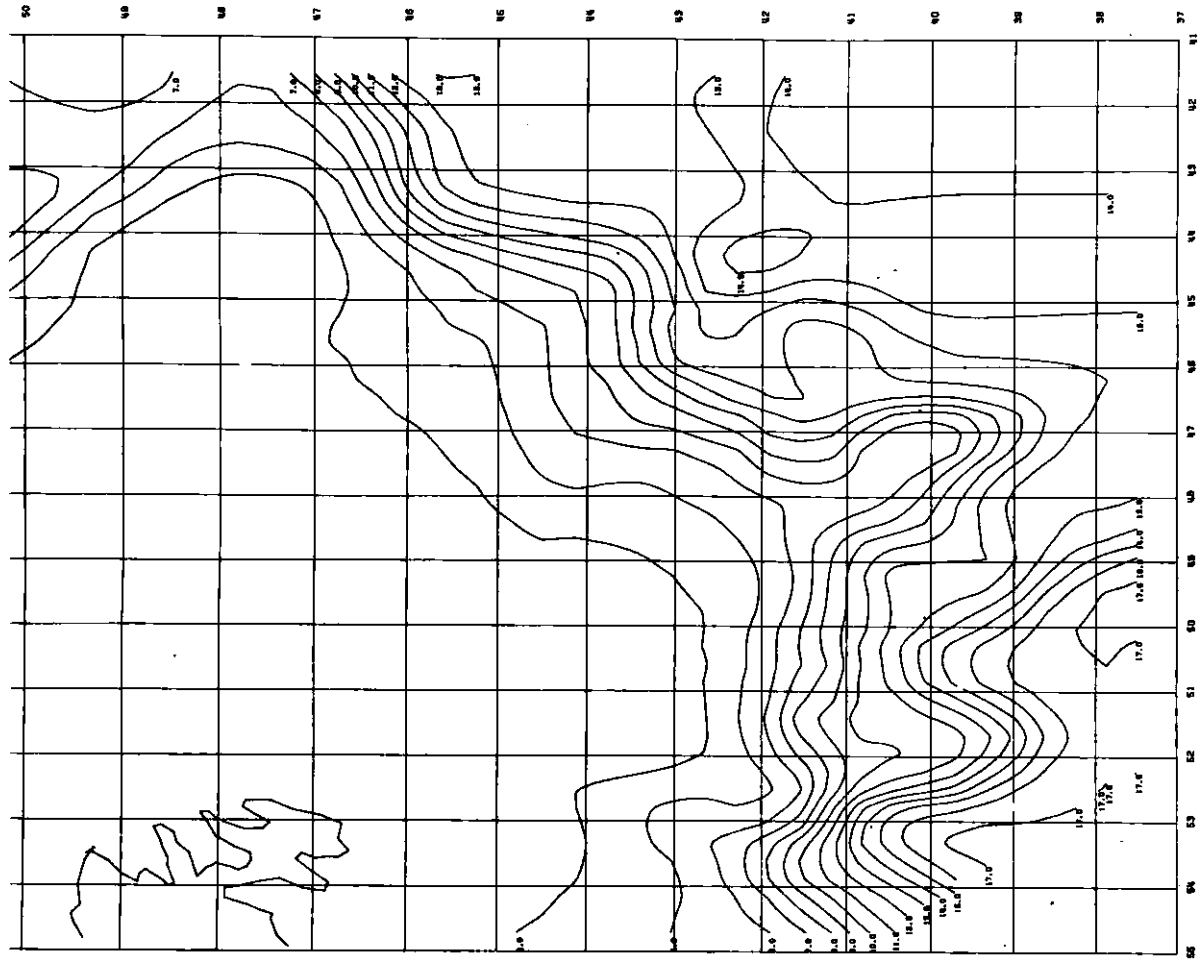


ICRAF AREA 400 METER TEMPERATURE

Figure 16. Horizontal plot of mean 400-meter temperature for February. Note: Some contours are erroneous, occurring where the depth is less than 400 meters.

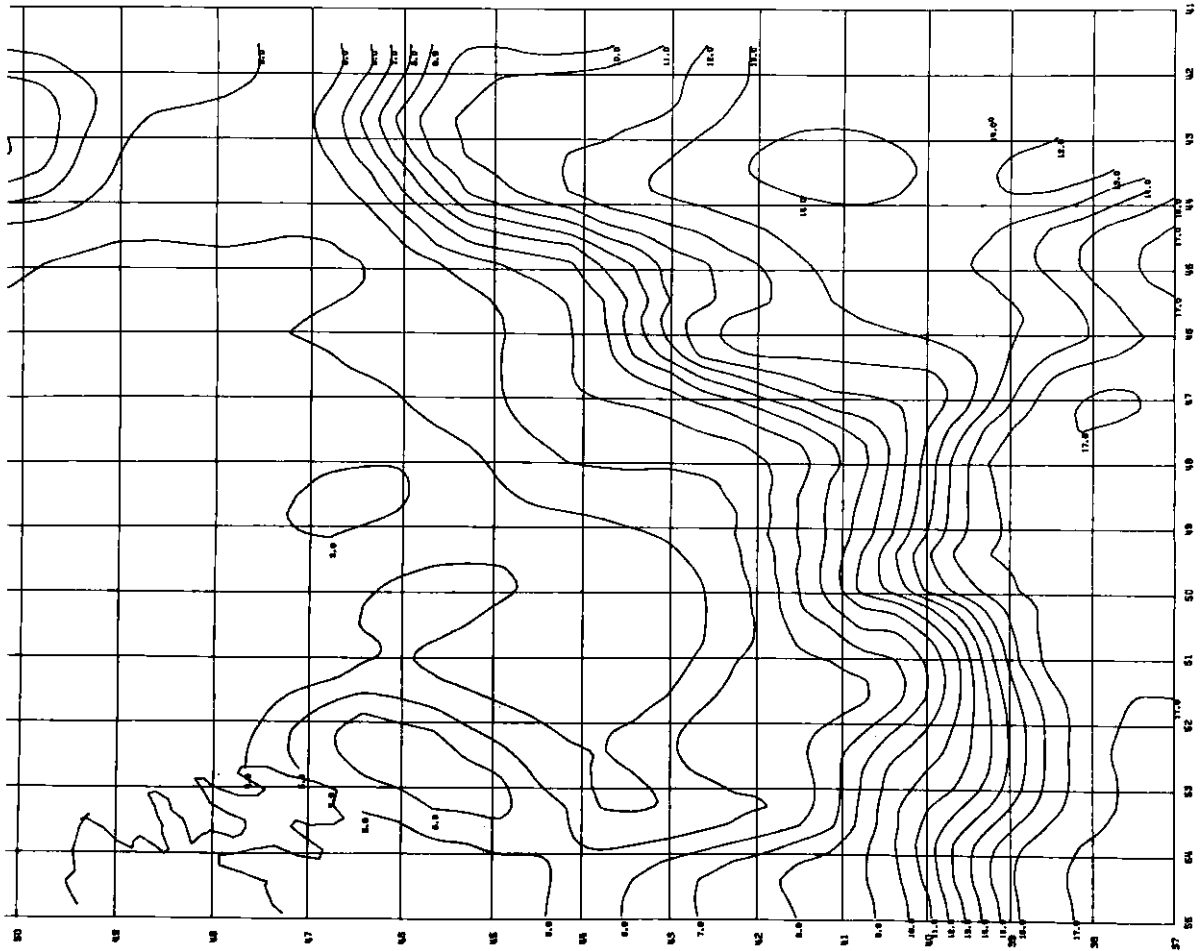
ICRAF AREA 400 METER TEMPERATURE

Figure 17. Horizontal plot of mean 400-meter temperature for March. Note: Some contours are erroneous, occurring where the depth is less than 400 meters.



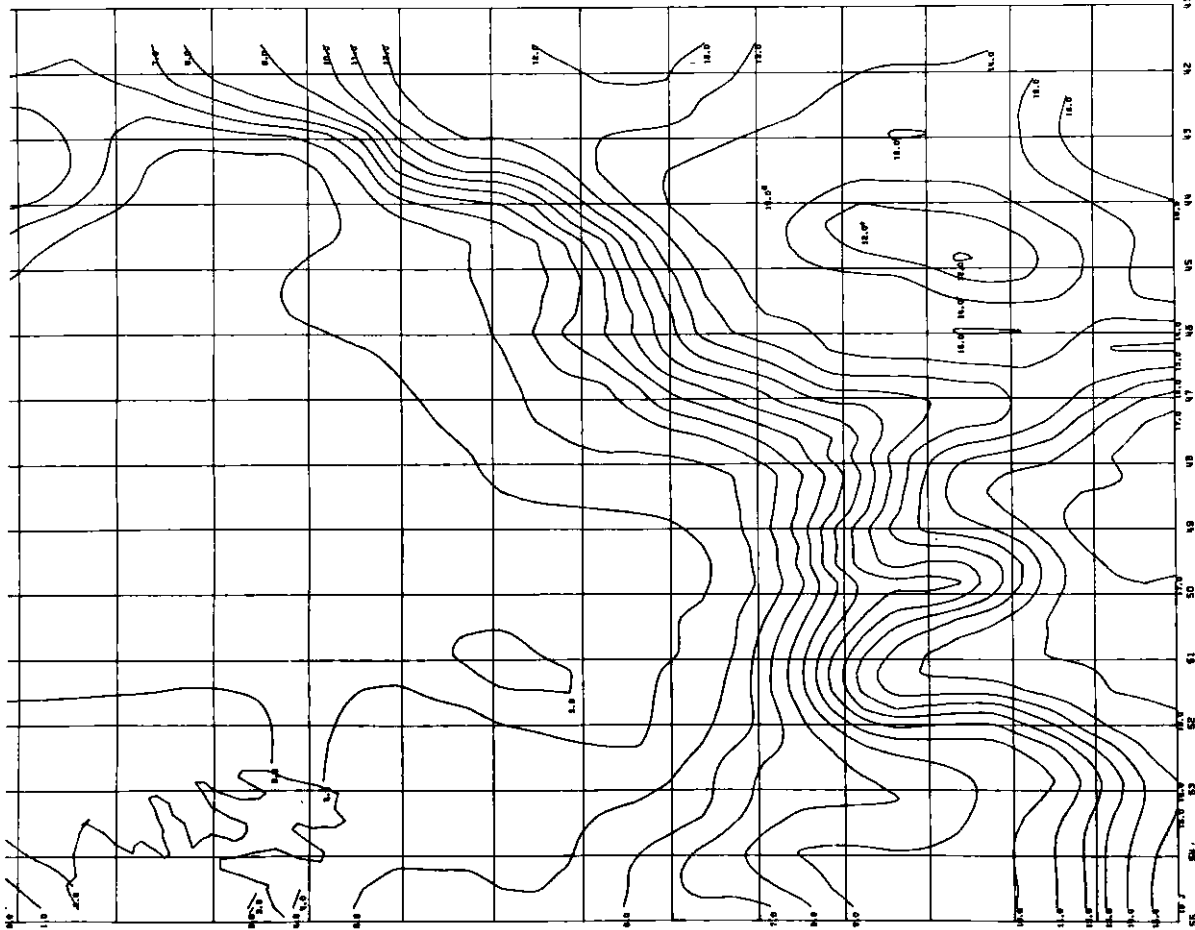
ICMRF AREA 400 METER TEMPERATURE

Figure 18. Horizontal plot of mean 400-meter temperature for April. Note: Some contours are erroneous, occurring where the depth is less than 400 meters.



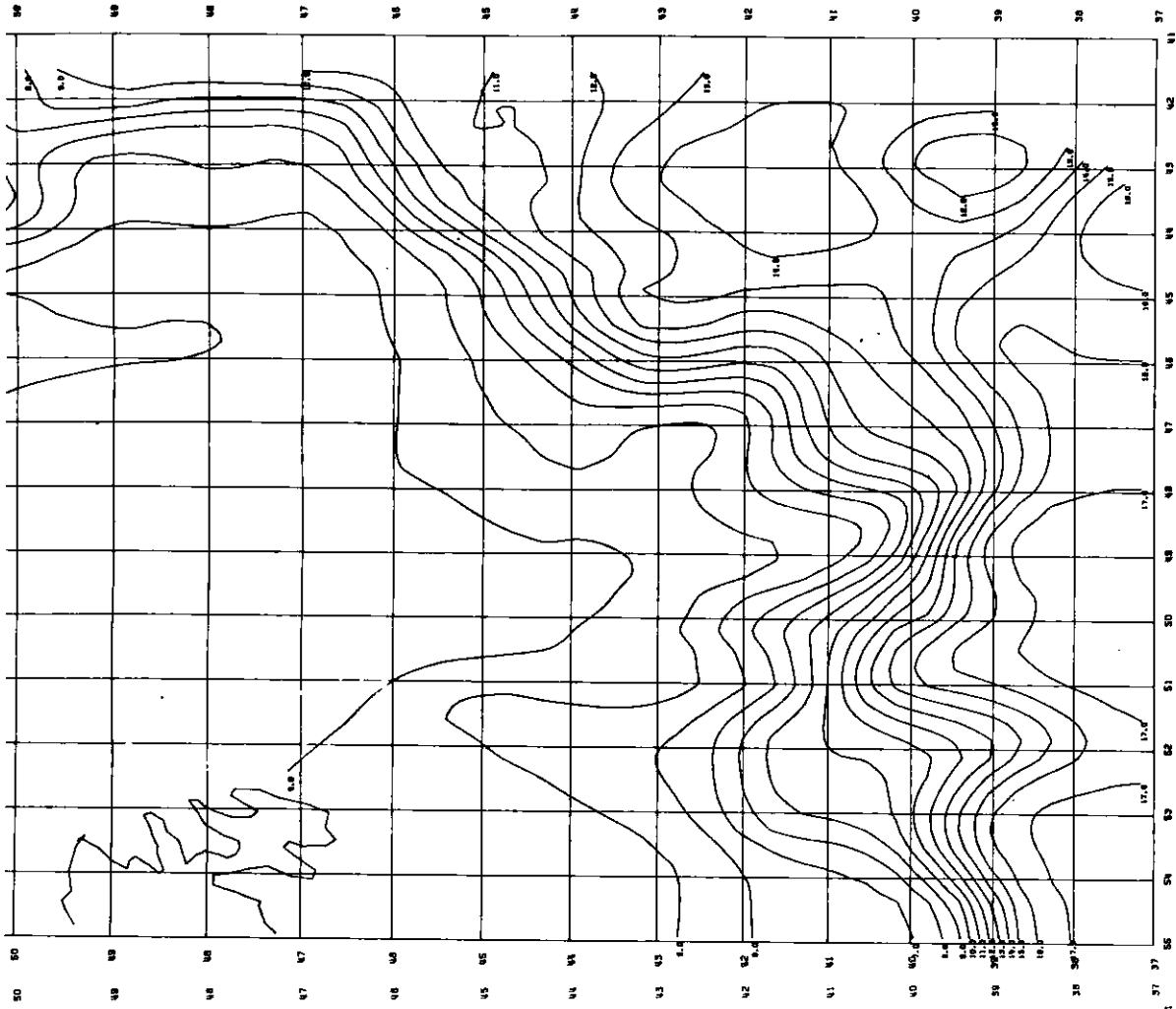
ICMRF AREA 400 METER TEMPERATURE

Figure 19. Horizontal plot of mean 400-meter temperature for May. Note: Some contours are erroneous, occurring where the depth is less than 400 meters.



ICRAF AREA 400 METER TEMPERATURE

Figure 20. Horizontal plot of mean 400-meter temperature for June. Note: Some contours are erroneous, occurring where the depth is less than 400 meters.



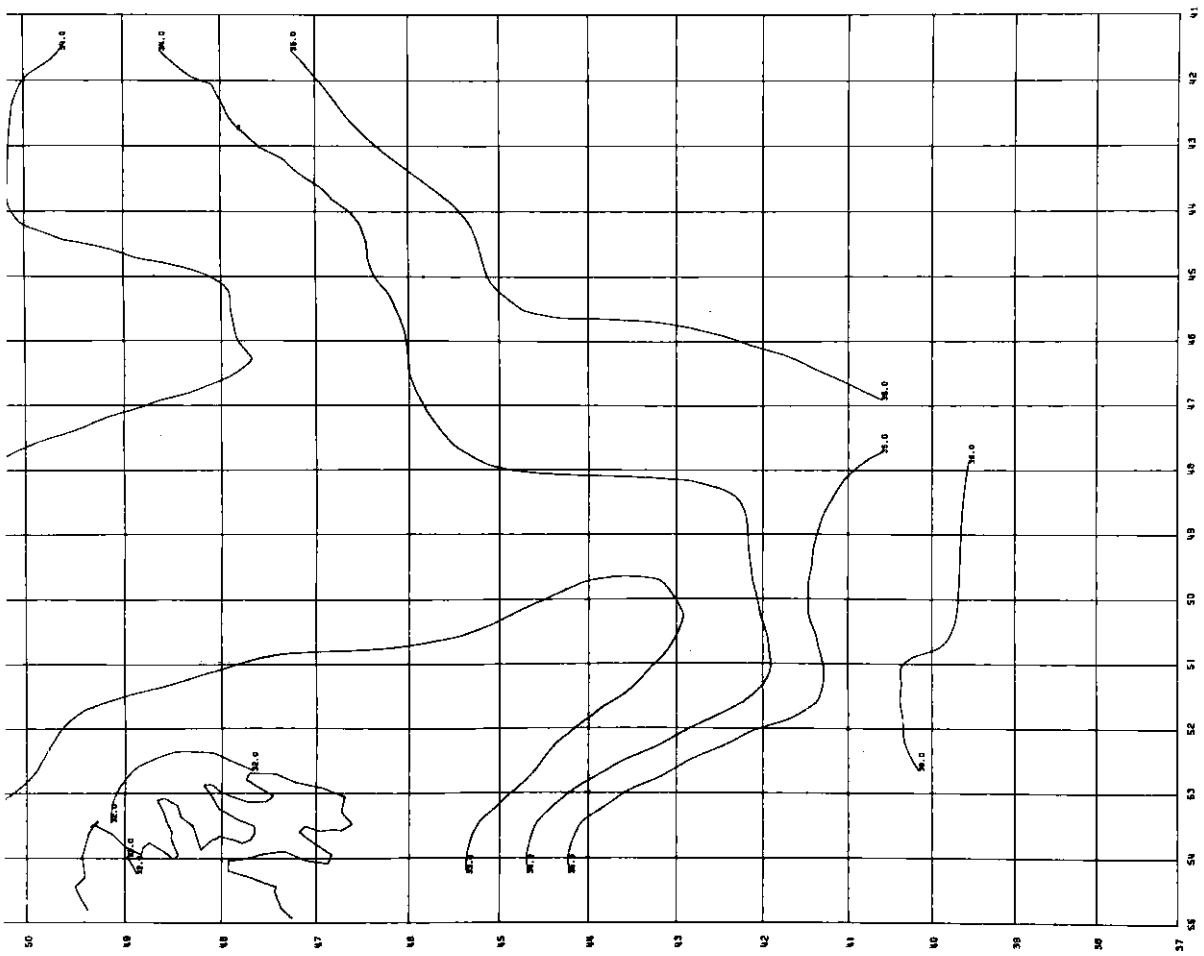
ICRAF AREA 400 METER TEMPERATURE

Figure 21. Horizontal plot of mean 400-meter temperature for July. Note: Some contours are erroneous, occurring where the depth is less than 400 meters.



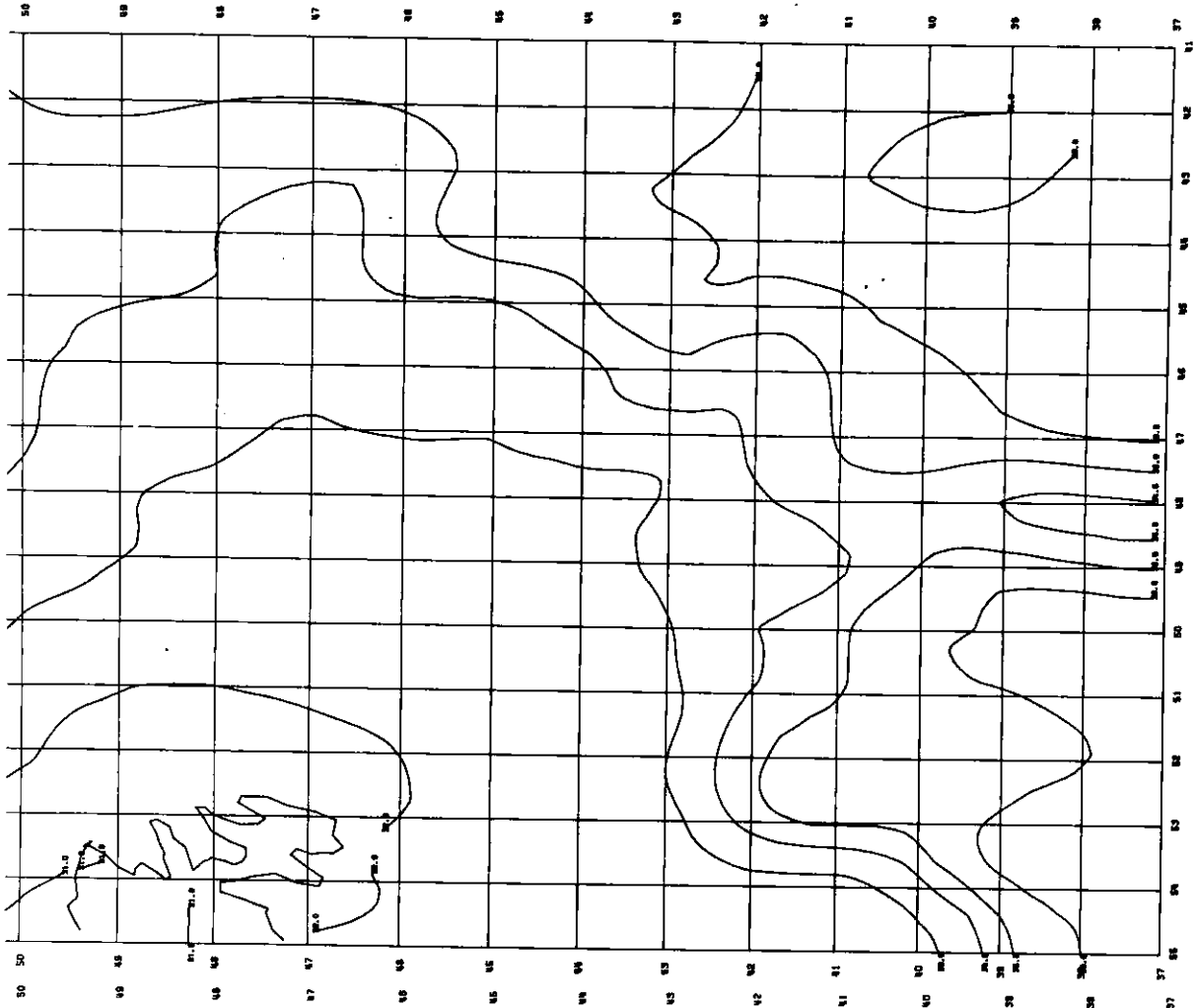
ICNAF AREA SURFACE SALINITY

Figure 23. Horizontal plot of near surface salinity for March.



ICNAF AREA SURFACE SALINITY

Figure 22. Horizontal plot of near surface salinity for February.



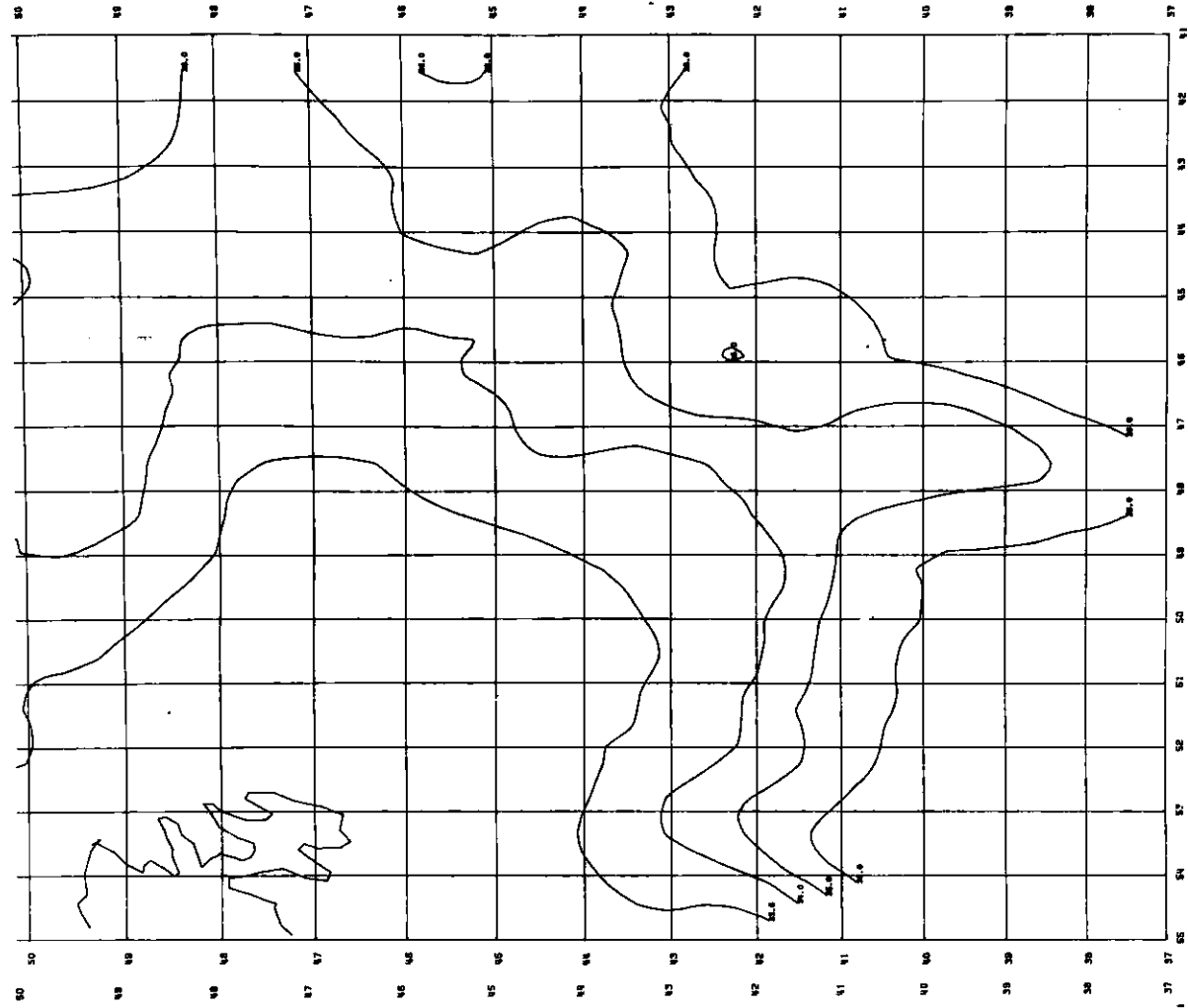
ICRAF AREA SURFACE SALINITY

Figure 27. Horizontal plot of near surface salinity for July.



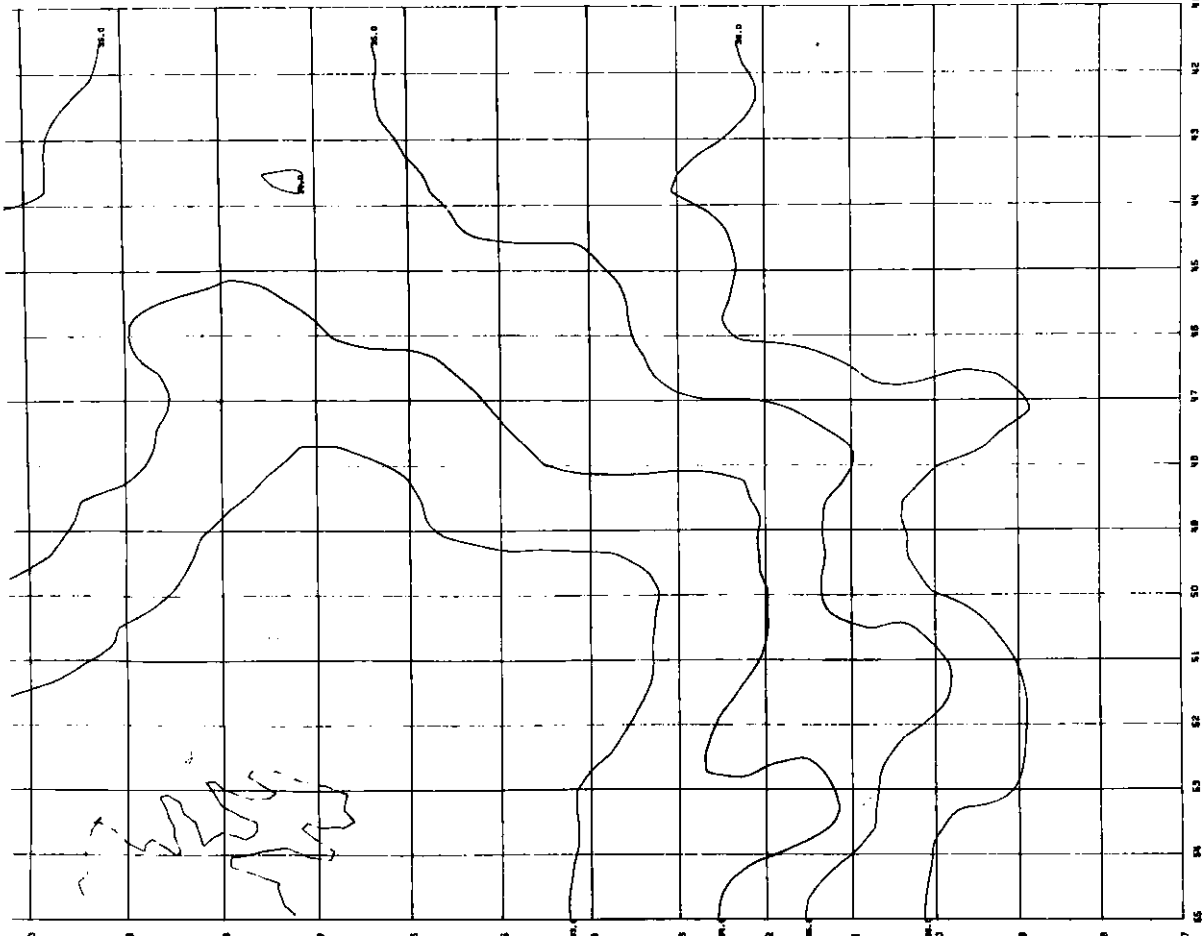
ICRAF AREA SURFACE SALINITY

Figure 26. Horizontal plot of near surface salinity for June.



ICRAF AREA SURFACE SALINITY

Figure 25. Horizontal plot of near surface salinity for May.



ICRAF AREA SURFACE SALINITY

Figure 24. Horizontal plot of near surface salinity for April.

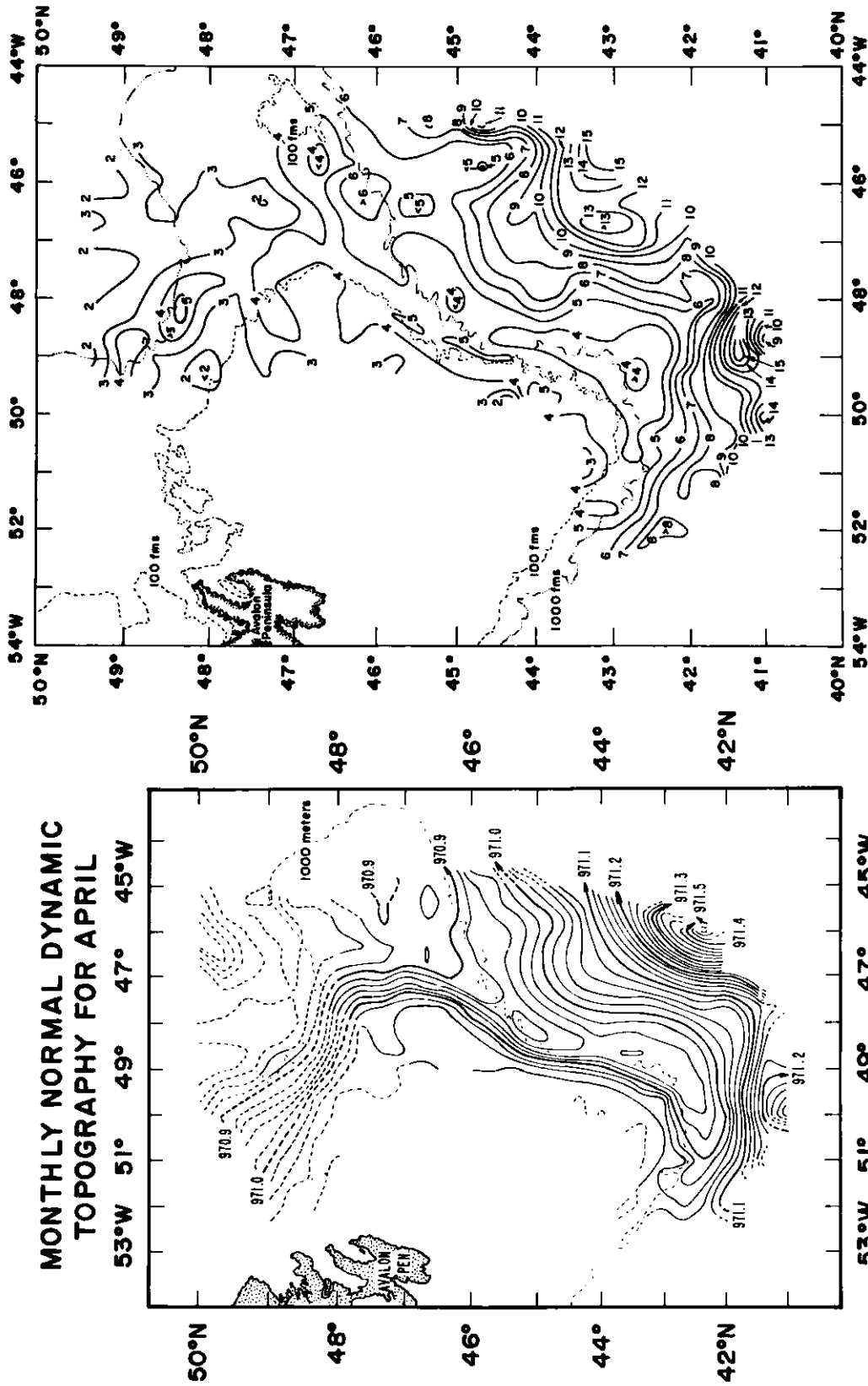


Figure 28a. April normal dynamic topography of the sea surface relative to the 1000 decibar level. Dynamic topographies are based upon 32 years of oceanographic data (from Scobie and Schultz, 1976).

Figure 28b. Field of standard deviation of dynamic height of the individual surveys from the April normal. Contour level is 1 dynamic centimeter.

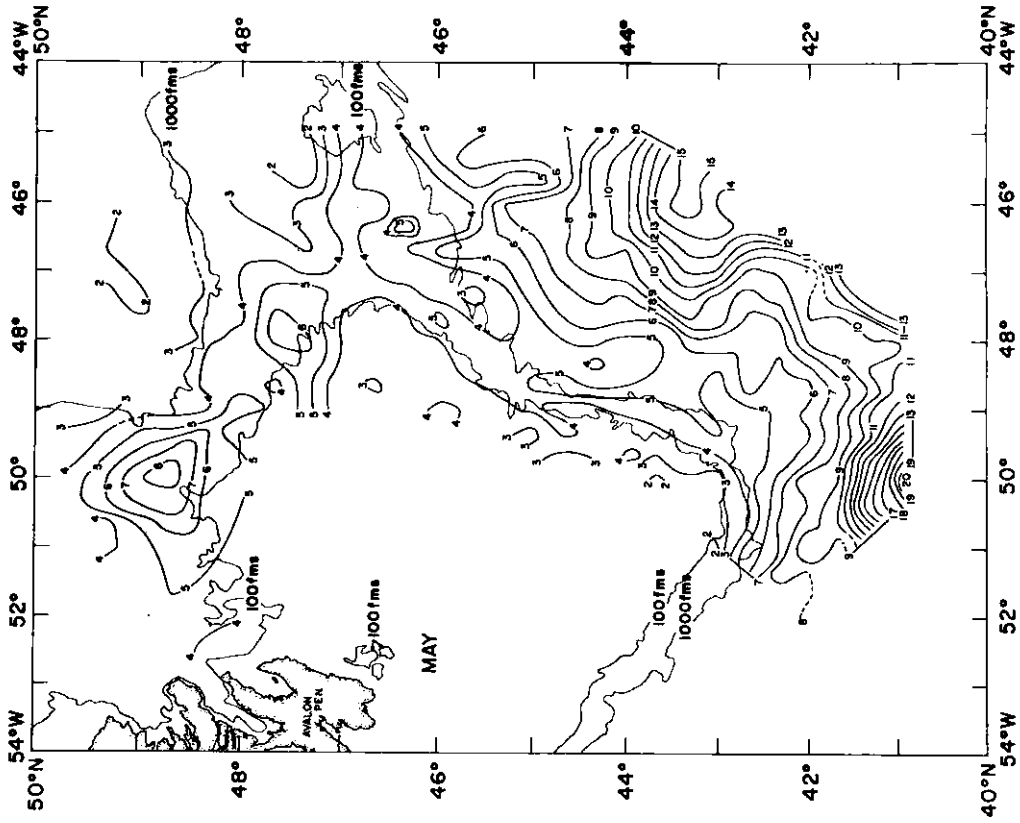


Figure 29a. May normal dynamic topography of the sea surface relative to the 1000 decibar level. Dynamic topographies are based upon 32 years of oceanographic data (from Scobie and Schultz, 1976).

**MONTHLY NORMAL DYNAMIC TOPOGRAPHY FOR MAY**

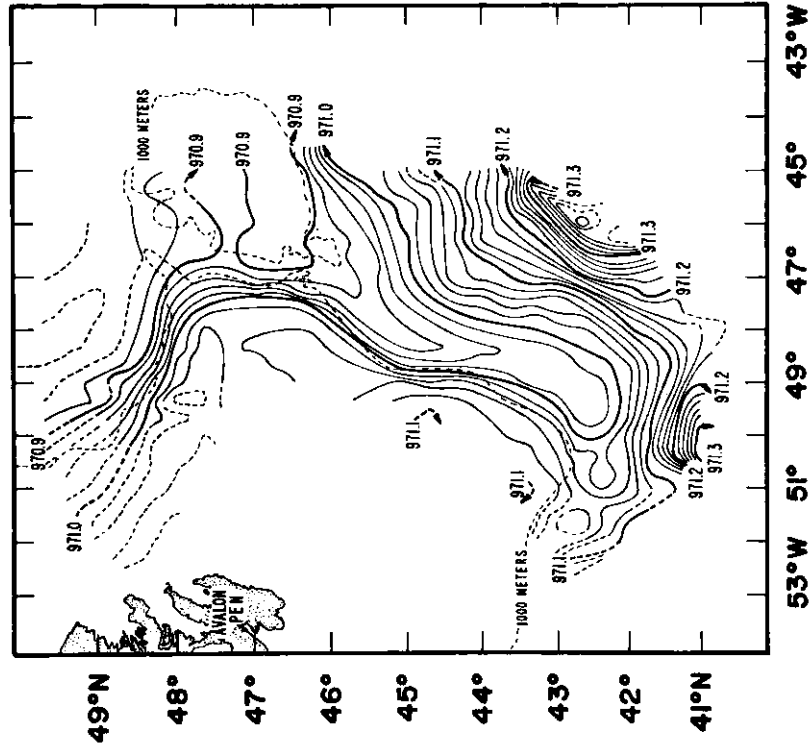


Figure 29b. Field of standard deviation of dynamic height of the individual surveys from the May normal. Contour level is 1 dynamic centimeter.

**MONTHLY NORMAL DYNAMIC  
TOPOGRAPHY FOR JUNE**

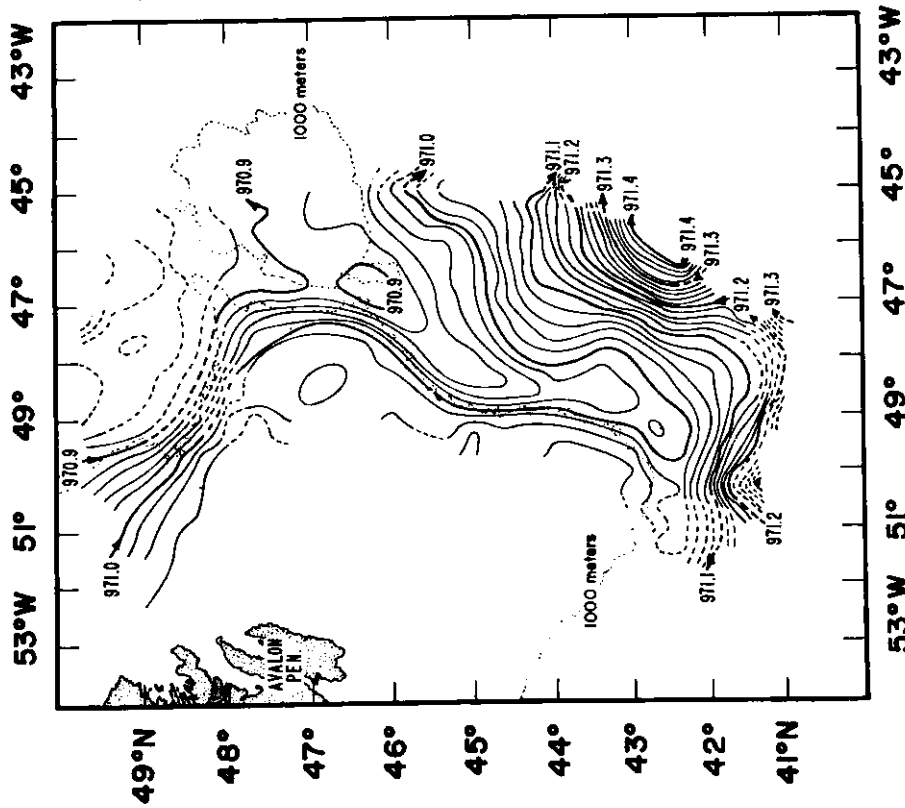


Figure 30a. June normal dynamic topography of the sea surface relative to the 1000 decibar level. Dynamic topographies are based upon 32 years of oceanographic data (from Scobie and Schultz, 1976).

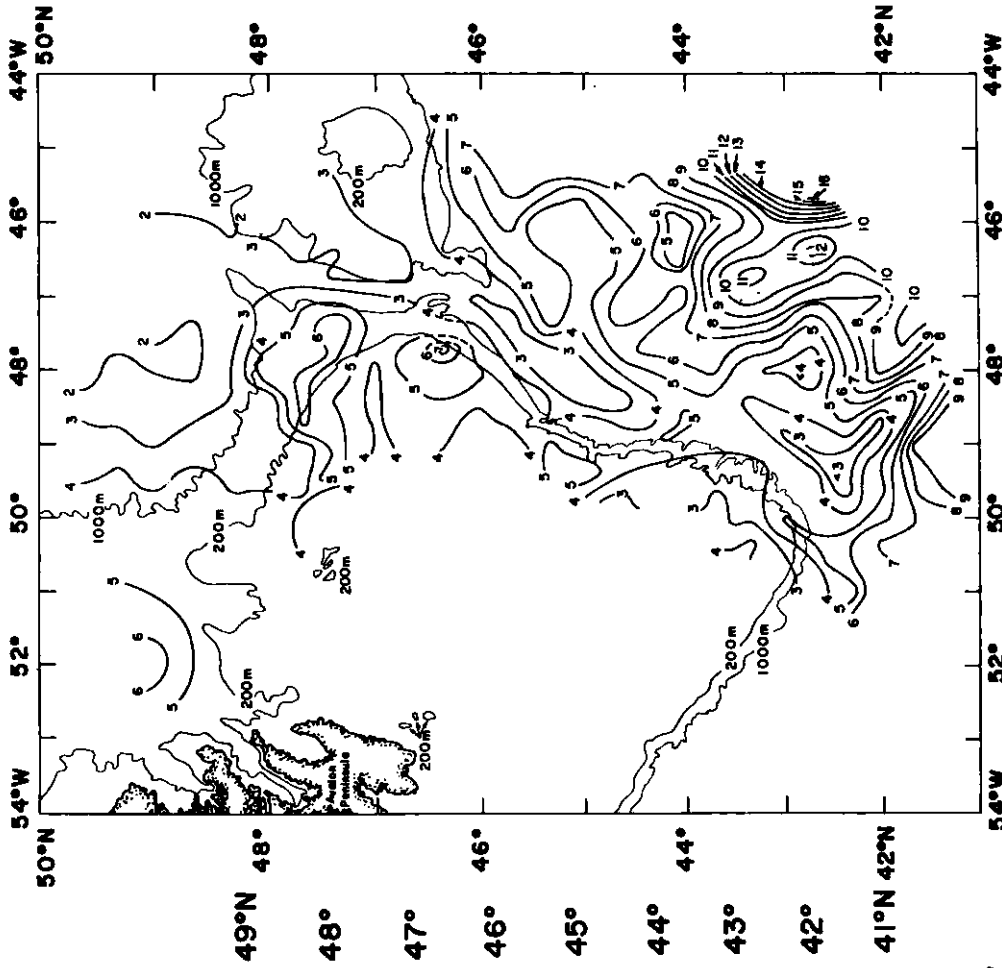


Figure 30b. Field of standard deviation of dynamic height of the individual surveys from the June normal. Contour level is 1 dynamic centimeter.

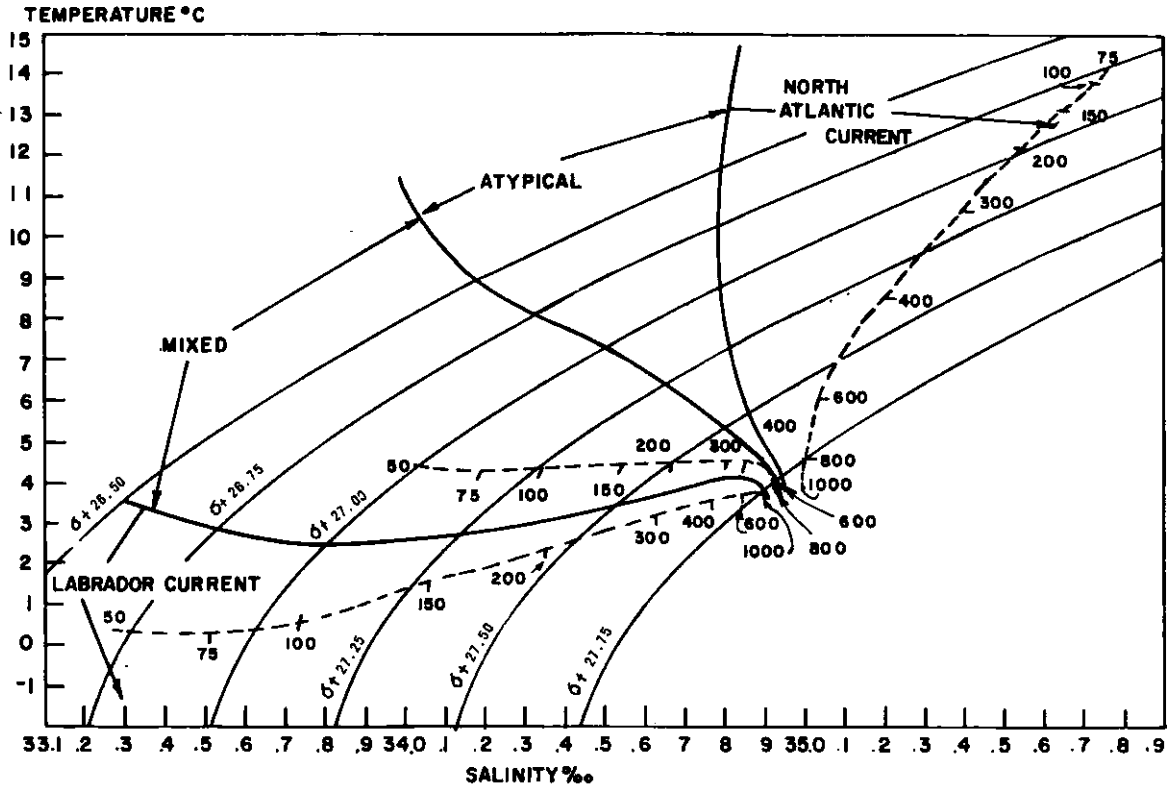


Figure 31. Criteria to determine the water masses found near the Grand Banks of Newfoundland. The dashed line represents a 20-year mean for each water mass.

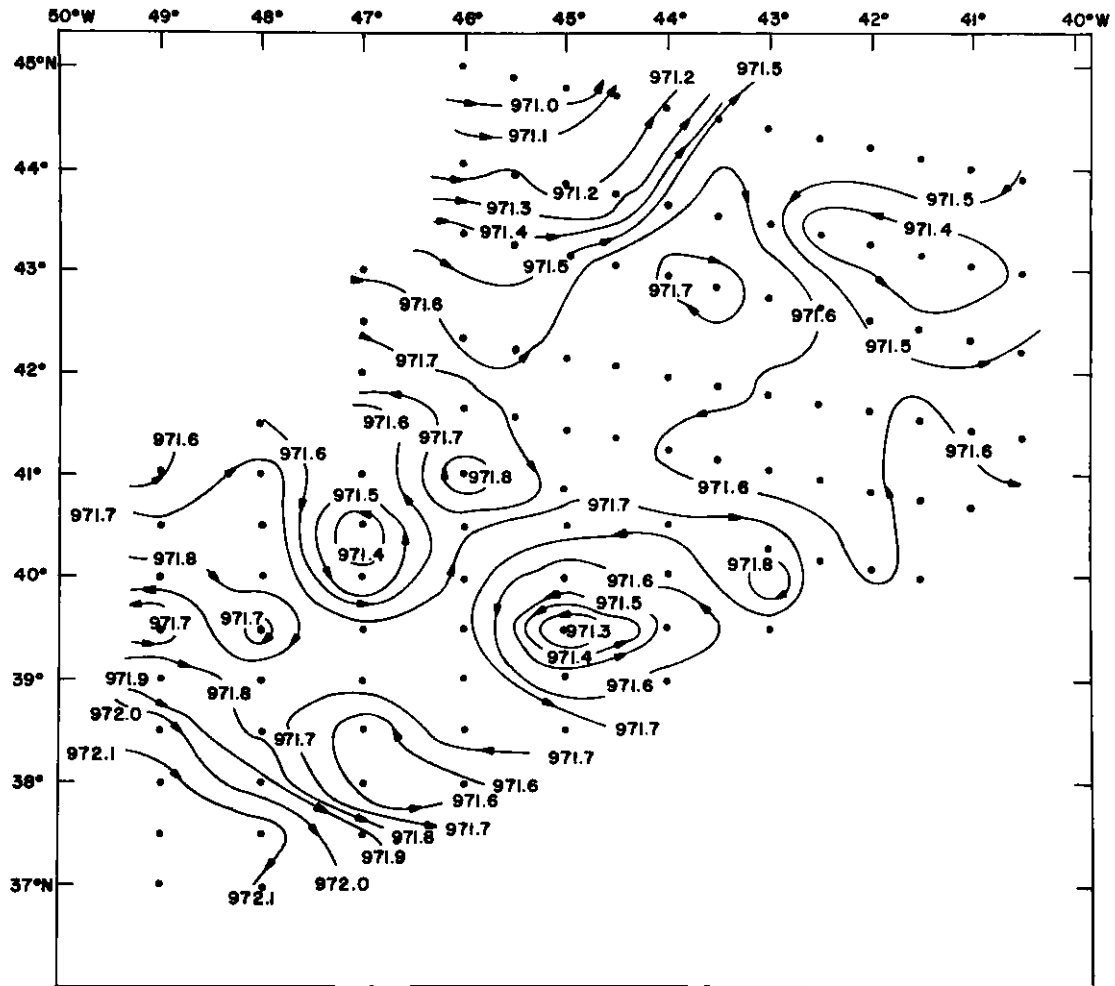


Figure 32. Dynamic topography of the sea surface relative to the 1000 decibar reference level, from data collected 10 to 25 June, 1976 by the USCGC SHERMAN. Dots represent oceanographic station locations.

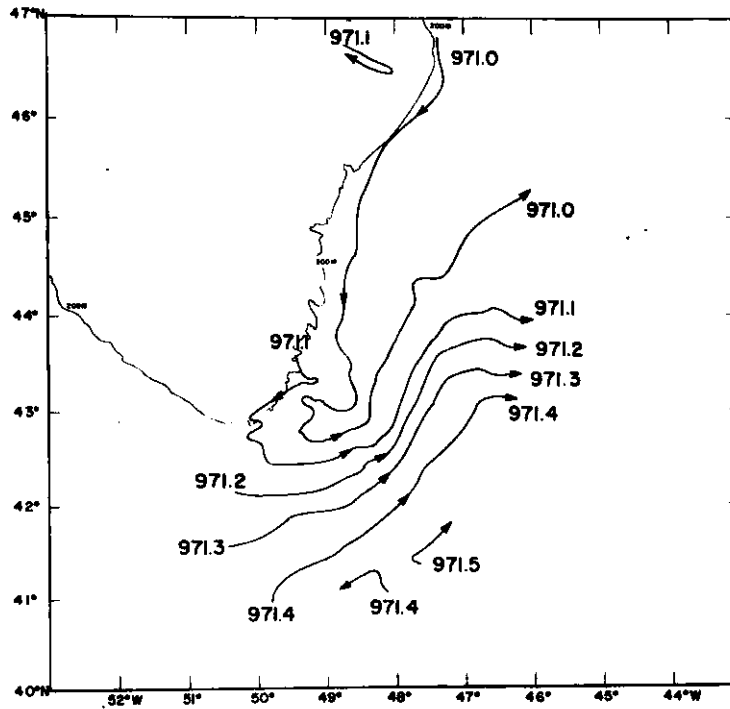


Figure 33. Dynamic topography of the sea surface relative to the 1000-decibar reference level, from data collected 8 to 20 June by the USCGC EVERGREEN.

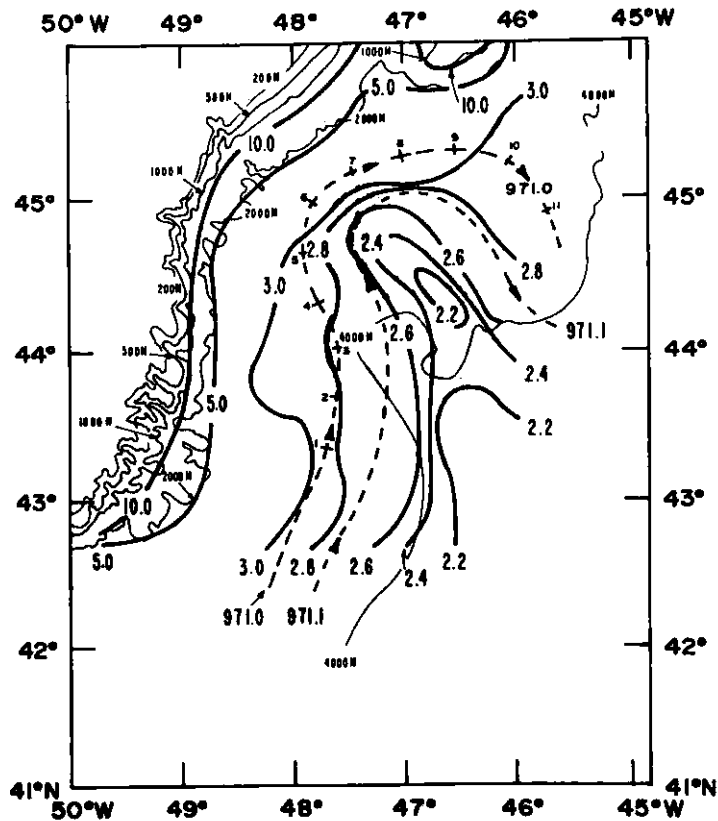


Figure 34. Potential vorticity (solid line in  $10^{-8}m^{-1}s^{-1}$ ) and dynamic height (dashed line in dynamic meters) contours derived from oceanographic station data collected 9-19 June 1964 by the USCGC EVERGREEN.

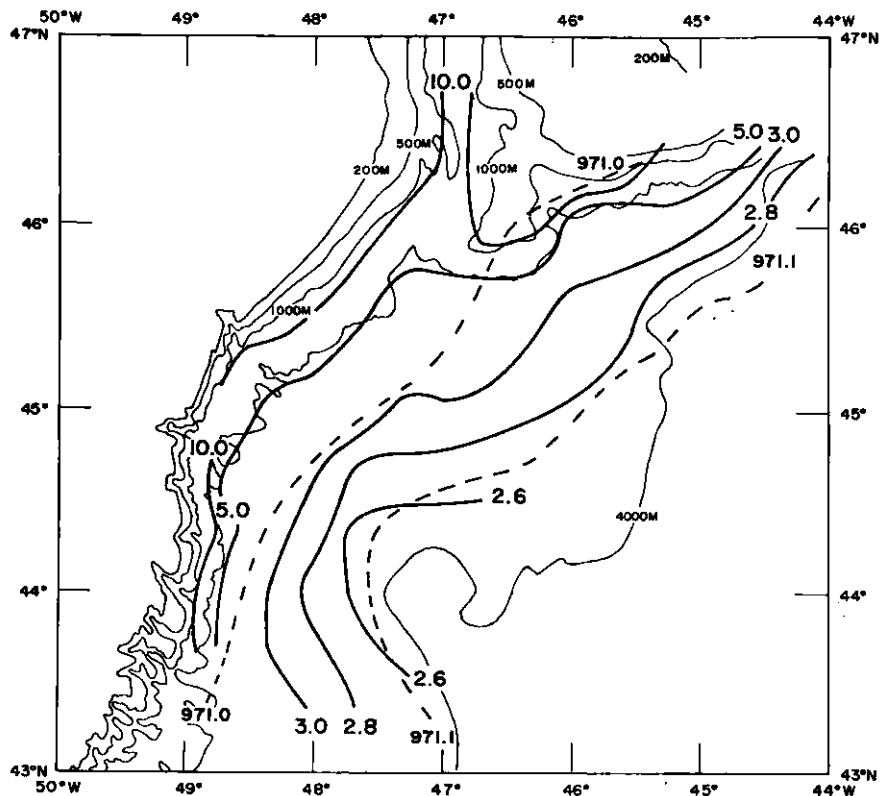


Figure 35. Potential vorticity (solid line in  $10^{-8} \text{ m}^{-1} \text{ s}^{-1}$ ) and dynamic height (dashed line in dynamic meters) contours derived from oceanographic station data collected 5-13 April 1971 by the USCGC EVERGREEN.

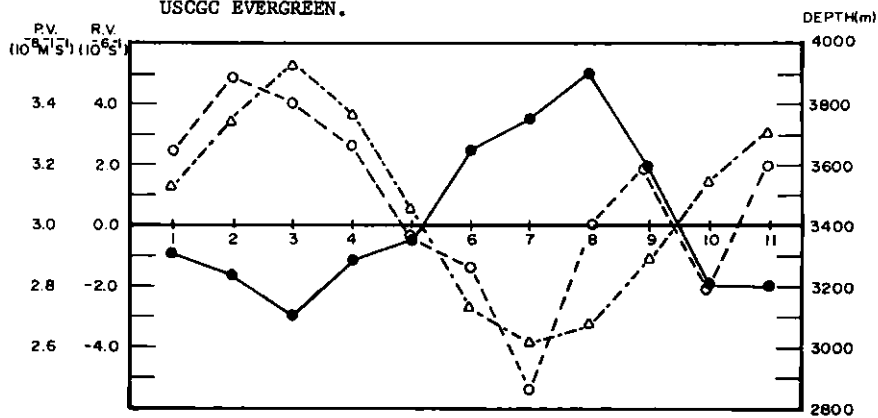


Figure 36. Potential vorticity ( $10^{-8} \text{ m}^{-1} \text{ s}^{-1}$ ) (—•—), relative vorticity ( $10^{-6} \text{ s}^{-1}$ ) (o---o), and depth (m) ( $\Delta$ -- $\Delta$ ) at numbered points along the flow path in Fig. 34.

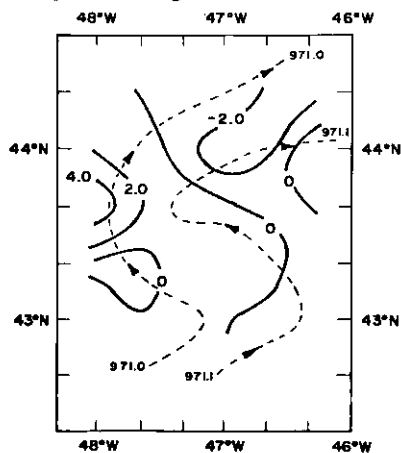


Figure 37. Vorticity tendency ( $10^{-11} \text{ s}^{-1}$ ) (—) and dynamic topograph in dynamic meters (---) from data obtained 2-13 May 1964 by the USCGC EVERGREEN.

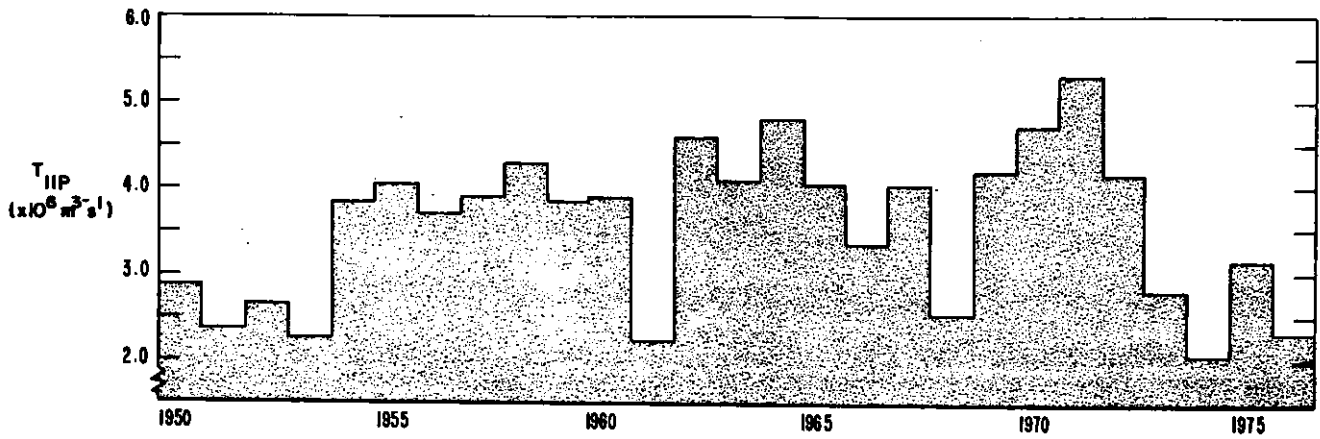


Figure 38a. Yearly averaged Labrador Current volume transports through sections T and U (near sections A2B and A3 respectively in Fig. 1a.) for the period 1950-1976.

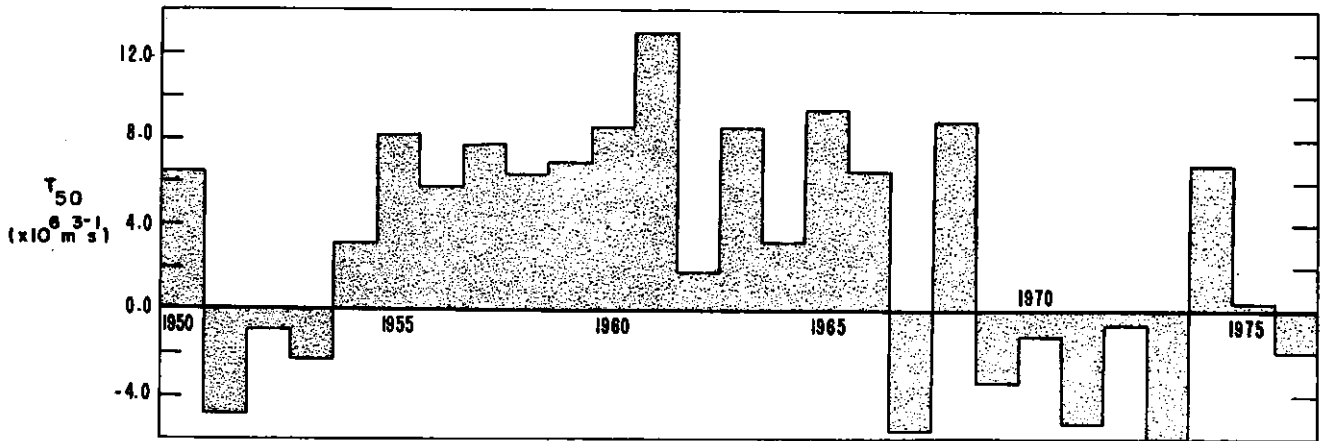


Figure 38b. Yearly averaged volume transports of the Labrador Current at 50°N, 50°W determined from wind stress curl calculations.

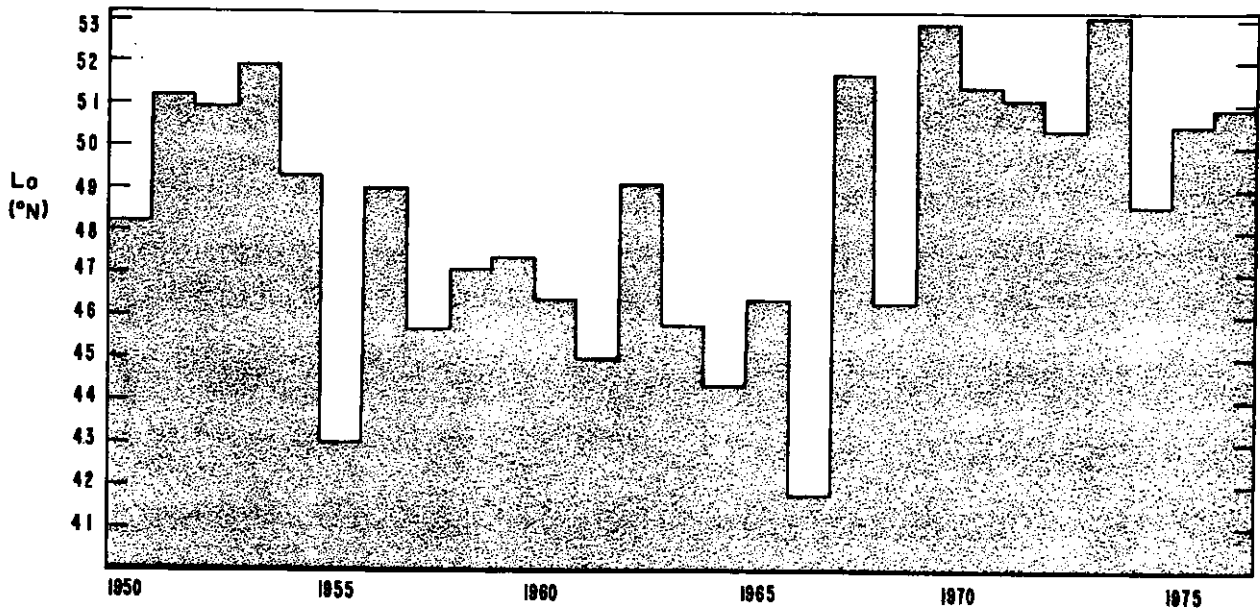


Figure 38c. Calculated latitude of the zero volume transport contour ( $L_0$ ) along the 45°W meridian.

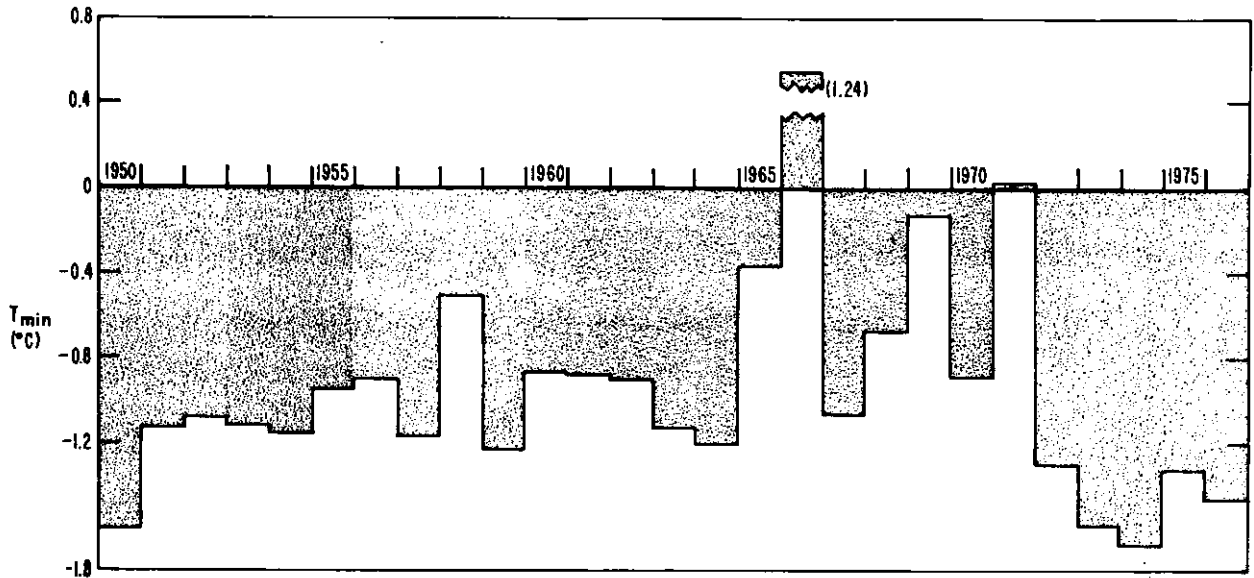


Figure 39a. Yearly averaged minimum temperatures for all occupations of sections T and V for the period 1950-1976.

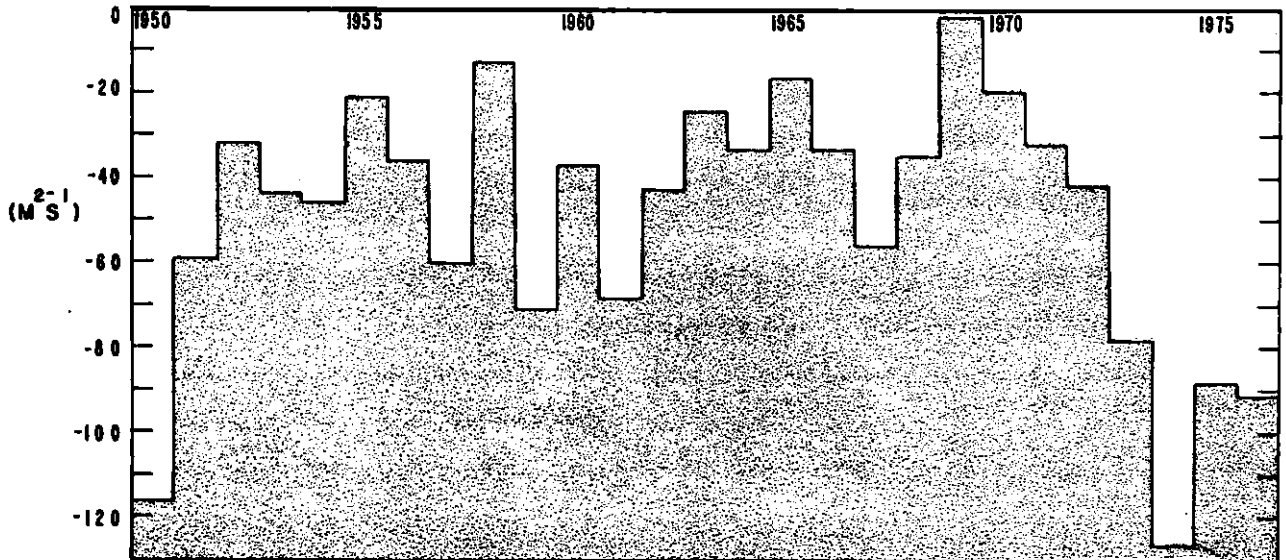


Figure 39b. South westerly Ekman transports along the Labrador coast at  $55^{\circ} N$ ,  $55^{\circ} W$  averaged for the months January, February, and March.

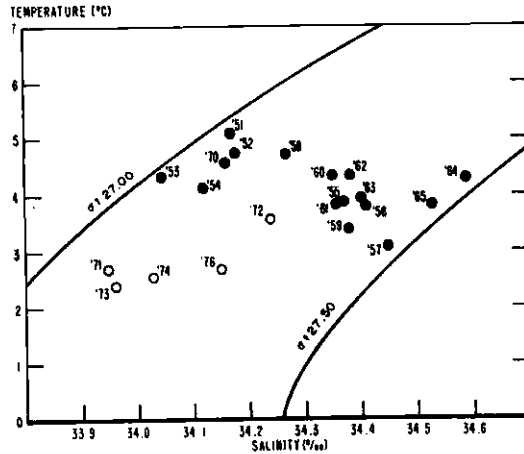


Figure 40a. Temperature-Salinity diagram of the 0 to 200 meter layer in the area 46° 40' - 47°N, 45° - 46° W on the southwestern side of Flemish Cap.

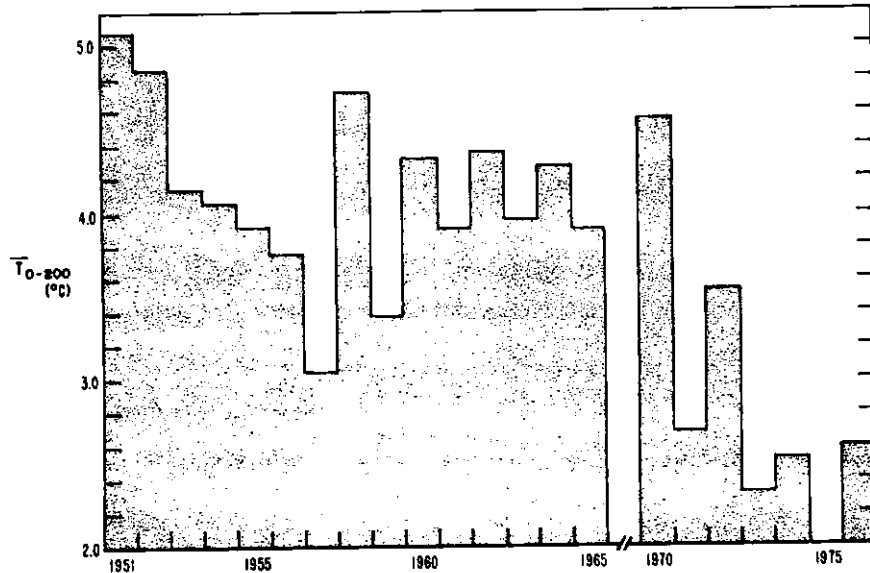


Figure 40b. Weighted mean temperature of the 0 to 200 meter layer located in the area 46° 40' - 47° N, 45° - 46° W on the south side of the Flemish Cap.

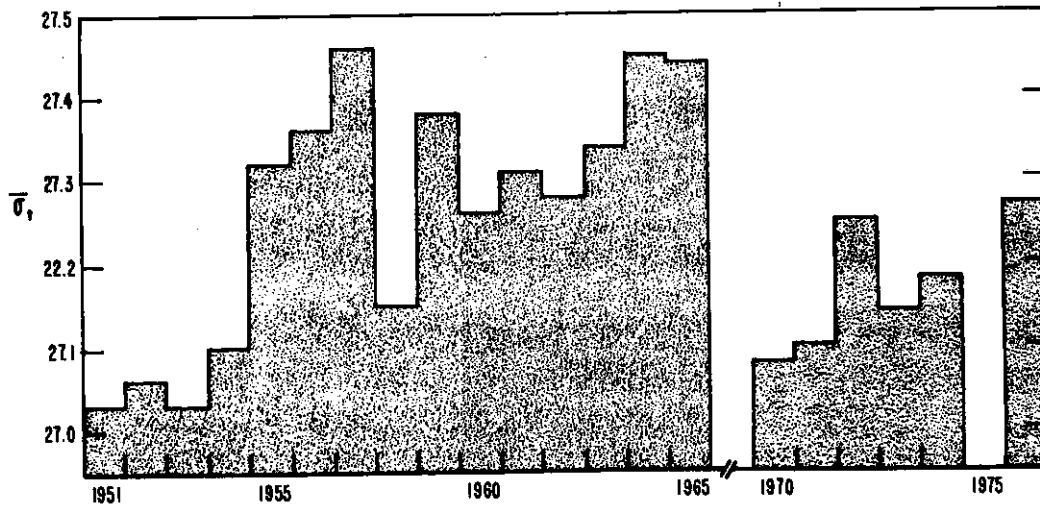


Figure 40c. Weighted mean density of the 0-200 meter layer located in the area 46° 40' - 47°N, 45° - 46°W on the southwestern side of Flemish Cap. The weighted mean sigma-t is computed from weighted mean values of temperature and salinity.

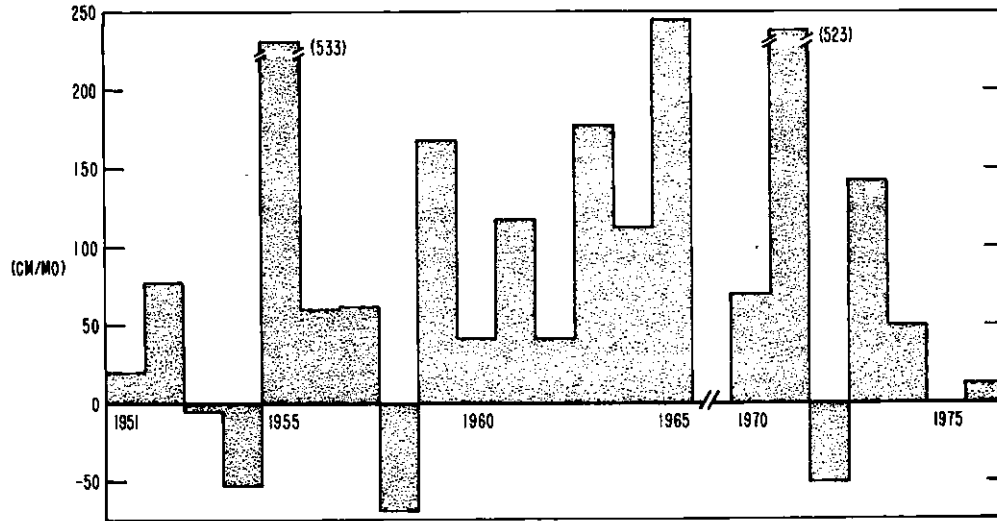


Figure 41a. Calculated vertical velocity produced by the divergence of the Ekman transport.

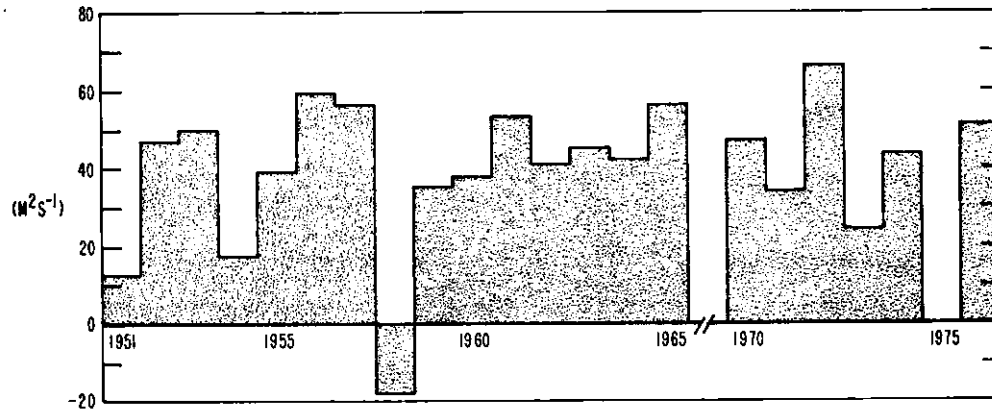


Figure 41b. The southeastern Ekman transport at 45° N, 45° W averaged over April to June.

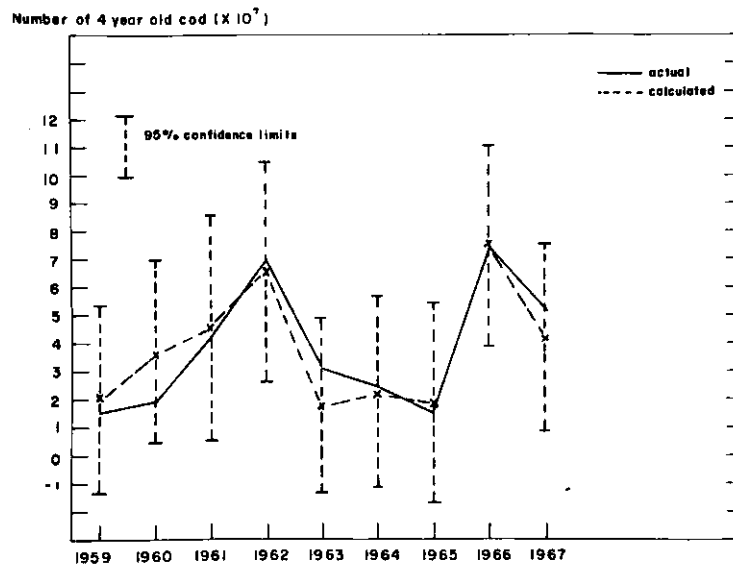


Figure 42. Comparison of actual versus calculated estimate of recruitment of 4 year old Cod on Flemish Cap (ICNAF Division 3M), 1959-1967.

